

# Embedded solids of any dimension in the X-FEM.

## Part II - Imposing Dirichlet boundary conditions

F. Duboeuf and E. Béchet

*University of Liège, Aerospace & Mechanical Engineering Department - Computer-aided Geometric Design,  
Allée de la Découverte 9, B-4000 Liège, Belgium*

---

### Abstract

This paper focuses on the design of a stable Lagrange multiplier space dedicated to enforce Dirichlet boundary conditions on embedded boundaries of any dimension. It follows a previous paper in a series of two, on the topic of embedded solids of any dimension within the context of the extended finite element method. While the first paper is devoted to the design of a dedicated P1 function space to solve elliptic equations defined on manifolds of codimension one or two (curves in 2D and surfaces in 3D, or curves in 3D), the general treatment of Dirichlet boundary conditions, in such a setting, remains to be addressed. This is the aim of this second paper. A new algorithm is introduced to build a stable Lagrange multiplier space from the traces of the shape functions defined on the background mesh. It is general enough to cover: (i) boundary value problems investigated in the first paper (with, for instance, Dirichlet boundary conditions defined along a line in a 3D mismatching mesh); but also (ii) those posed on manifolds of codimension zero (a domain embedded in a mesh of the same dimension) and already considered in Béchet *et al.* 2009. In both cases, the compatibility between the Lagrange multiplier space and that of the bulk approximation (the dedicated P1 function space used in (i), or classical shape functions used in (ii)) —resulting in the inf-sup condition— is investigated through the numerical Chapelle-Bath test. Numerical validations are performed against analytical and finite element solutions on problems involving 1D or 2D boundaries embedded in a 2D or 3D background mesh. Comparisons with Nitsche's method and the stable Lagrange multiplier space proposed in Hautefeuille *et al.* 2012, when they are feasible, highlight good performance of the approach.

**Keywords:** Embedded solids, Extended finite element method, Dirichlet boundary condition, Lagrange multipliers, P0-equivalent space, stability, inf-sup condition

---

*E-mail:* [frederic.duboeuf@gmail.com](mailto:frederic.duboeuf@gmail.com), [fduboeuf@ulg.ac.be](mailto:fduboeuf@ulg.ac.be) (F. Duboeuf); [eric.bechet@ulg.ac.be](mailto:eric.bechet@ulg.ac.be) (E. Béchet).

*Preprint submitted to Finite Elements in Analysis and Design*  
*Article accepted for publication* DOI:[10.1016/j.finel.2017.01.005](https://doi.org/10.1016/j.finel.2017.01.005)

*July 30, 2016*  
*January 17, 2017*

**Contents**

<b>1</b>	<b>Introduction</b>	<b>2</b>
1.1	Background . . . . .	5
1.2	Objectives . . . . .	11
1.3	Outline . . . . .	12
<b>2</b>	<b>Model problem</b>	<b>12</b>
2.1	Weak formulations . . . . .	14
2.2	Finite element discretisation . . . . .	15
<b>3</b>	<b>Design of the stable Lagrange multiplier space</b>	<b>19</b>
3.1	Terminology . . . . .	19
3.2	Description of the algorithm . . . . .	20
<b>4</b>	<b>Numerical validations</b>	<b>23</b>
4.1	Dirichlet constraints on an embedded line in 2D . . . . .	25
4.2	Dirichlet constraints on an embedded line in 3D . . . . .	28
4.2.1	Unit-square of codimension one . . . . .	28
4.2.2	Unit-cube of codimension zero . . . . .	31
4.3	Dirichlet constraints on an embedded surface in 3D . . . . .	35
4.3.1	Sinusoidal field with a Dirichlet constraint on an embedded planar surface . . . . .	36
4.3.2	Logarithmic field with a Dirichlet constraint on an embedded spherical surface . . . . .	40
<b>5</b>	<b>Conclusion</b>	<b>42</b>

**1. Introduction**

One of the basic principles common to most finite difference, Finite Element (FE) and finite volume methods is the discretisation of the *physical domain* on which the problem to solve is defined. The mesh — consisting of elements supporting the shape functions — must

generally conform to the boundaries of the domain, thus forcing the geometric description to be identical to the support of the function space. Although h- or p-refinement can increase the accuracy of the results, this dependency leads to tedious mesh generation tasks that are often done manually.

While interest in solving problems with complex and evolving geometry has seen a huge momentum, the constraint of using a conforming mesh remains a critical issue. The physical domain evolution may result in major changes in shape and topology during the simulation, due to some physics that need to be described and solved on the discretisation. This highly non-linear problem requires to remesh at each iteration before solving PDEs. In order to address this, two families of methods have emerged. One can cite meshless and particle methods based on lattice nodes alone [1, 2, 3], which quite substantially modify the FE computational kernel. On the other hand, eXtended Finite Element Method (X-FEM)-like approaches are improvements of the classical FEM. Thus, they are less intrusive and allow to keep most of the qualities of the FEM approach, while allowing non-matching meshes. In this paper, we will focus on the latter methods, for which the connectivities obtained with the mesh give a straightforward way to satisfy the Kronecker delta property to the shape functions.

In context of the FE method, this paradigm — to dissociate the field approximation and the boundary representation — raises the following issues:

- (i) Use a convenient representation of the geometry with regard to the FE method.
- (ii) Find an appropriate function space built from the classical FE shape functions.
- (iii) Enforce Boundary Conditions (BCs) on embedded boundaries, with a singular focus on Dirichlet BCs. Neumann BCs cause no problems in this case.

The X-FEM has taken advantage of the flexibility offered by Partition of Unity Methods (PUM) [4, 5] in the generation of meshes. Classically, the FE mesh discretisation has the same dimension as the problem domain, but without having to conform to boundaries such as those describing e.g. a crack.

Although this method can be combined equally well with an explicit or implicit geometric

representation, the choice of appropriate tools such as Level Sets [6, 7] allows to describe cracks [8, 9, 10, 11], or complex geometries [12] with great flexibility. It also allows to define the possible enrichment functions (modelling the discontinuity and the solution at the crack tip), to evolve and propagate the crack.

Then, the FE shape functions defined over the bulk mesh are simply used as function space and the elements intersected by an interface — called *parent elements* — are partitioned into sets of *sub-elements* for integration purposes (such as in Figure 1).

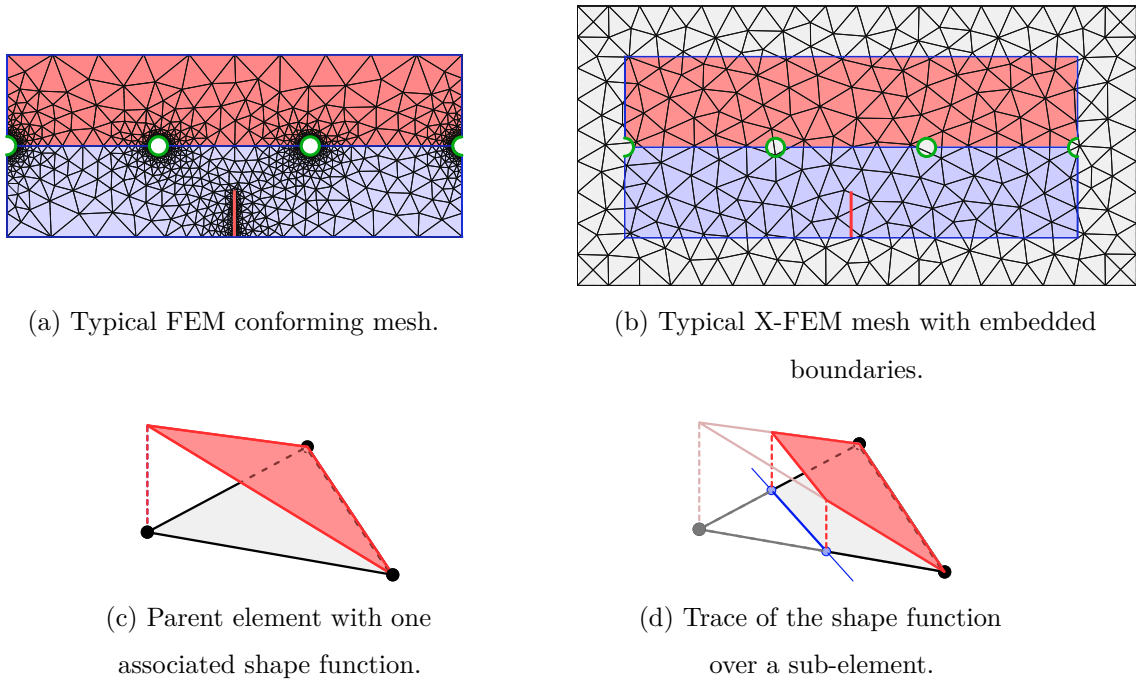


Figure 1: FEM and X-FEM discretisations of a domain with different types of interface.

Zoom over one parent element with its subdivision into sub-elements.

But the enforcement of boundary conditions on boundaries crossing the elements requires special attention. Adding Neumann type BCs remains as straightforward as in the standard finite element method, whereas the enforcement of Dirichlet type BCs is more tricky.

- With a Neumann BC enforced on an implicit boundary, or a traction-free condition, the variational formulation of the X-FEM does not introduce additional terms. Only the

integration over the sub-elements describing the interface differs from the conforming case. Such an approach is not new, and optimal convergence rate is preserved even with curved boundaries, despite the use of unfitted meshes as shown in [13].

- To impose a Dirichlet BC in the standard FE method consists in eliminating the degrees of freedom (DOFs) associated with the nodes along the boundary, because of interpolating shape functions. It is not suitable in case of a boundary not entirely matched by the mesh, where shape functions are no more interpolating.

In this study, we will focus on the enforcement of Dirichlet type BCs — and more broadly, stiff conditions used to accurately transfer fluxes between two domains glued together — in the context of the X-FEM. Problems involving domains of a higher codimension will also be investigated, as surfaces embedded in a 3D mesh, thanks to dedicated P1 function spaces introduced in a preliminary paper [14]. A detailed review of such other techniques dealing with embedded problem is also presented in that paper.

### *1.1. Background*

There are different ways in which a boundary value problem along an embedded boundary can be handled. We give an overview of approaches available in the literature and allowing to impose Dirichlet BCs in this setting.

The naive approach is such that the physical domain is reduced to the elements identified as being entirely within the boundaries and the narrow band of elements intersected by them is lost. Although easy to implement, this approach leads to errors of order  $h$ , the size of discretisation.

An alternative consists in locally modifying the mesh when the elements are cut by the interface. This local boundary-fitting remeshing approach includes, for instance, the Universal Meshes developed in two [15] and three dimensions [16] and local anisotropic mesh adaptation [17]. However, although beneficial to the prescription of boundary conditions with nodal collocation, remeshing — even just locally at the boundaries — causes drastic change in topology, with higher computational cost to rebuild the mesh connectivity and to project

the solution of a moving boundary problem between two time steps. This calls for other alternatives based on non-conforming meshes independent of the geometry of the problem.

The simplest approach would be to choose a test function space already including the boundary condition. Unfortunately, standard basis functions having a support crossed by the interface do not necessarily satisfy the boundary condition. They must therefore be replaced. Because only constant functions on the boundaries are optimally approximated with this approach, the results are then sub-optimal, and not better than using the naive approach. An illustration of this is presented in [18], showing a locking-type phenomenon. Most of the approaches that are subsequently described relax the Dirichlet condition to avoid locking, enforcing this BC in a weak sense.

A strategy to impose Dirichlet BCs on a non-conforming mesh consists in changing the approximation close to the interfaces. The boundary-fitting interpolation can be achieved in two different ways:

- i) to modify the interpolation space. Codina and Baigues propose in [19, 20] to approximate in a weak sense the boundary value problem, by the extrapolation of DOFs near the boundaries. The sub-elements do not use the shape functions of the parent element, but an extension of the shape functions of neighbouring elements interior to the domain, which are not cut.
- ii) to introduce a specific enrichment of the interpolation space by including new unknowns along the boundary. A first attempt would be to enrich the elements intersected by the interface, in the way of the Generalised Finite Element Method (GFEM) and X-FEM. However, the necessity of blending elements to avoid pollution from higher order shape function has been an issue. Indeed, by using local enrichment at the nodes of elements crossed by the boundary, the neighbouring elements are also affected because of the continuity of the shape functions across the interface between two elements.

To tackle this problem, one approach is to enrich only the points of intersection of the boundary with the edges of the mesh. Thus, the enrichment functions vanish at the vertices of the mesh. Their supports will be limited to the band of cut elements.

This approach developed in [21, 22] for the case of multi-material and known as the I-GFEM (Interface-GFEM), takes its name from the shift of the new DOFs — called generalised DOFs — to the interfaces. The enforcement of a Dirichlet BC can be done in the classical way of the FEM, using collocation technique thanks to the DOFs and/or generalised DOFs on the interface [23]. However, it is still quite sophisticated to build the enrichment functions, as it depends on interface/element configurations. In order to overcome this difficulty, a hierarchical approach was recently used in the case of multiple interfaces within a single element [24].

Another possibility of enrichment can be achieved by switching to discontinuous interpolants in the cut elements. The discretisation is based on the Discontinuous Galerkin technique [25, 26], but limited to the narrow band of elements that intersect the boundary [27, 28]. In contrast with the weakly continuous approaches, the Dirichlet conditions remain strongly enforced in this case.

More recently, a two-field approach [29] introduces also piecewise discontinuous functions in the elements cut by the interface and vanishing elsewhere. It is based on the mixed stress-displacement formulation in relation to the Hellinger-Reissner variational principle. The additional stress unknowns are replaced by their expression in the primary displacement field through a condensation technique applied at the discrete level along the boundaries. Although the resulting system contains only the primary unknowns, it leads to unsymmetric linear system, even for symmetric problems. To preserve a symmetric elliptic problem, the formulation has been symmetrised in [30, 31] and extended to high-order embedded domain discretisations [32].

One final strategy to enforce Dirichlet BCs is to change the formulation in the elements crossed by the interface. Along an interface that is not conforming to the mesh, a stiff boundary/interface condition can be taken into account through a force term. For instance, in a fluid-structure interaction, such additional term appears in either the strong or the weak form of the boundary value problem. Variety of methods have been proposed in the literature and may be classified according to the way of prescribing the condition:

- i) to add point-wise spring forces using a Dirac-delta function along the interface. Peskin had introduced this approach in its original form in [33], later known as the Immersed Boundary Method (IBM). But difficulties arise in the transition of the continuous problem to the discretised problem, only leading to a first-order accurate approach. In the continuous case, the enforcement of the condition should require an unbounded linear feedback control limited to the interface. But after discretisation, a thick regularisation zone and a finite parameter must be used to prevent ill-conditioning. To achieve optimal second-order accuracy, an Immersed Interface Method (IIM) has been depicted in [34, 35, 36, 37] and defines the forcing term without the requirement of Dirac-delta distribution.
- ii) to define a purely numerical forcing term. A penalty term is introduced in [38] with a mesh-dependent parameter and analysed for embedded boundaries in [39]. Penalty methods are similar to Peskin's methods by adding one term in the formulation; however the latter remains localised on the thin interface. In tandem with the good approximation of the boundary condition, the contribution of the test functions associated to the boundary nodes must be taken into account to obtain a good approximation of the solution fields. To this end, Nitsche [40] proposed the introduction of another term to improve the previous method. The symmetry of the problem can then be retrieved thanks to additional terms in the formulation. Unfortunately, the formulation involves a parameter that is also dependent on the physical problem. Although the proof of the stability of Nitsche's method for general boundary conditions is done in [41], this parameter should be carefully selected in order to get a stable formulation. To avoid choosing a parameter, efforts have been done in [19], but the resulting formulation remains non-symmetric in every case. Another variant of Nitsche's method [42, 43] tends to the unconditional stability at the expense of higher regularity requirements in comparison with the standard method. Moreover, these studies are limited to two-dimensional problems. The application to three-dimensional problems has been made in [44] with convergence studies. The parameter is computed with analytical

expressions at the element level [45, 46]. Furthermore, if the physical domain exhibits material non-linearities and/or evolving interface, Nitsche's method may sometimes be difficult to apply.

- iii) Lagrange multipliers may be introduced to represent the fluxes on the boundary. The solution of the boundary value problem is then obtained by moving to a dual formulation. The design of the Lagrange multiplier space should be done with caution: a naive attempt is to use the space built on the boundary with piecewise linear shape functions at the intersections of the interface geometry with the edge of the bulk mesh. In two dimensions, rebuilding a submesh defined from the intersection of the interface with the bulk mesh is possible, it is however not suitable in a complex three-dimensional case. A convenient choice for the Lagrange multipliers is to simply use the traces of the primary shape functions defined on the mesh, restricted to the interface. Nevertheless, it has been observed either with the naive space [47] or the trace space [48, 49], that both cases lead to spurious oscillations of the Lagrange multipliers and locking. The domain integral smoothing technique [47] significantly improves the accuracy of the boundary flux by preventing the oscillations of Lagrange multipliers. But locking is not precluded and convergence properties remain sub-optimal. To circumvent these difficulties, the inf-sup condition and so-called Ladyzhenskaya-Babuška-Brezzi (LBB) compatibility condition proposed in [50, 51, 52, 53] must be satisfied by the pair of primal and dual finite element spaces.

Starting with an incompatible pair of spaces, a first solution consists in the stabilisation of the Lagrange multipliers. To this end, bubble shape functions may be added in order to build a stable approximation from an otherwise unstable Lagrange multiplier space. Brezzi *et al.* [54] has initially suggested to use bubble shape functions for domain decomposition. Introduced in [55] to enforce boundary conditions, this bubble-stabilised method has been improved in [56] by replacing simple cubic bubble functions by residual-free bubbles. Applications to adherence constraints are investigated in [57] and a comparison between penalty, Nitsche, unstable and stabilised space techniques is

made. This technique has the advantage of exhibiting no free parameters stabilisation compared to Nitsche's approaches, while preserving a positive-definite symmetric system. However, this requires to solve before an additional linear system in order to define the residual-free bubble functions. Instead of a stabilised space, the design of a stabilisation operator allows circumventing the inf-sup condition with a modification of the variational form, resulting in a stabilised formulation. A residual-based stabilisation is obtained by Barbosa and Hughes in [58, 59], by penalising the difference between the discrete normal derivative and the discrete Lagrange multiplier. Stenberg has established in [60] the close relationship to Nitsche's method. An optimal method is developed in [49] with a specific treatment of DOFs having a very small support intersection with the domain, for robustness purposes. Another operator is introduced in an interior penalty stabilisation by Burman [61] to penalise the jump of the Lagrange multipliers between elements. More recently, a local projection stabilisation is used in [62, 63] with a coarsening operator. Only Lagrange multipliers are involved through the operator, by penalising the distance between the full P1 space to an *a priori* stable space. At the end, the number of independent DOFs will be reduced to that of the stable space. This technique is more flexible to address non-linear problem than the initial Barbosa-Hughes stabilised method. However, it requires the prior identification of patches of elements for projection purposes, in order to have a coarse space satisfying the inf-sup condition.

A second solution requires a careful selection of a stable pair of spaces. To avoid an *a posteriori* recovery of the stability, the Lagrange multiplier space may be appropriately designed so as to pass the LBB condition. On the one hand, a separate interfacial mesh for the Lagrange multipliers has been introduced by Glowinski *et al.* in the fictitious domain method [64]. Optimal convergence is obtained in [65] with a uniform inf-sup condition, thanks to a wise choice of the ratio between the mesh size in the domain and the boundary mesh size. On the other hand, a stable Lagrange multiplier space may be carefully designed on a single bulk mesh. Starting with a space made up of

standard hat functions that is too rich, a first algorithm has been proposed in [18] to deplete the Lagrange multiplier space. A second algorithm has been introduced in [66] and extended for large sliding [67], improving the accuracy of the computed fields at the expense of the resolution of a global problem. Finally, a third algorithm [48] combines both a local construction of the Lagrange multiplier space and good accuracy. A theoretical analysis of the stability is performed in two dimensions. It uses the traces of primary shape functions to design the space and remains valid in 3D to enforce Dirichlet boundary condition on a surface. Hautefeuille *et al.* [44] compares a variant of this stable space with Nitsche's method. The specificity of the Lagrange multipliers in contrast to [48] lies in the local enforcement of the partition of unity at the element level. Then, discontinuities into the basis are allowed, introducing piecewise  $C_0$ -continuous shape functions. An advantage of Lagrange multipliers is the possibility to define precisely the coupling (contact or cohesive law), especially with non-linearities, something that is not easy with other methods (using Nitsche's and other stabilisation terms).

For all these approaches, studies have been limited to the case of Dirichlet constraints defined on submanifolds of codimension one. As we are going to see, this work continues the development of stable Lagrange multiplier approach.

### 1.2. Objectives

While the development of non-conforming approaches has shown a growing interest in last decades, solving problems posed on embedded surfaces has only been considered more recently in such settings. Nevertheless, the imposition of Dirichlet boundary conditions have not been yet addressed. In these cases, the embedding of a surface into the 3D ambient space defines a problem of codimension one. Then, the Dirichlet boundary is a submanifold of codimension two in 3D.

In the framework of stable Lagrange multipliers, the existing methods are not suitable for this type of constraint on implicit lines in 3D. They detect only intersection points of the boundary with edges of the mesh to design a suitable function space. Unfortunately,

1D boundaries are running, in 3D, through faces of most of the elements. A new method is therefore required. Furthermore, neither of the approaches presented before investigates this problem.

The aims of this paper can be summarised as follows:

1. Introduce a new algorithm designing stable Lagrange multiplier spaces on boundaries of arbitrary dimension in 2D and 3D, in order to address boundary value problems defined on manifolds of codimension zero, one or two.
2. Perform numerical convergence analyses with all configurations of boundary dimension, in order to show the accuracy, the optimality and the stability of the method.
3. Validate the results against classical FEM and compare with Nitsche's method wherever possible.

### 1.3. Outline

The outline of this paper is as follows. In the next section, we describe the governing equations of the model problem and its discretised forms. Then, Sect. 3 presents a new algorithm reducing the classical P1 Lagrange function space into a stable Lagrange multiplier space for every combination of the mesh and boundary dimensions. Several numerical examples and convergence studies are provided in Sect. 4 to investigate the performance of the method. Particular attention is placed on the comparison between the current approach and Nitsche's method. Finally, a summary and concluding remarks are given in the last section.

## 2. Model problem

Let  $\mathcal{T}$  be a Cartesian domain of dimension  $n = 1, 2$  or  $3$ , we consider the embedding into this ambient space of a bounded domain  $\Omega \subset \mathbb{R}^m$ , with  $1 \leq m \leq n$ . As model problem, we consider an elliptic equation with the same settings than in the preliminary paper [14].

If  $m = n$ , *i.e.* the codimension  $\text{codim}_{\mathcal{T}}(\Omega) := \dim \mathcal{T} - \dim \Omega$  is equal to zero, then the problem is simply a Poisson problem involving a Laplace operator and a source term  $f$ , otherwise a Laplace-Beltrami operator is introduced on  $\Omega$ .

To be succinct, we are combining both cases in a single formulation thereafter. To achieve this, we define for  $g : \mathcal{T} \rightarrow \mathbb{R}$  sufficiently smooth:

$$\nabla_{\Omega} g := \begin{cases} \nabla g & \text{if } \text{codim}_{\mathcal{T}}(\Omega) = 0, \\ \nabla g - \nabla g \cdot \mathbf{n}_{\Omega} \otimes \mathbf{n}_{\Omega} & \text{if } \text{codim}_{\mathcal{T}}(\Omega) = 1, \\ \nabla g \cdot \mathbf{t}_{\Omega} \otimes \mathbf{t}_{\Omega} & \text{if } \text{codim}_{\mathcal{T}}(\Omega) = 2. \end{cases} \quad (1)$$

Here,  $\mathbf{n}_{\Omega}$  and  $\mathbf{t}_{\Omega}$  are respectively the unit normal and tangent vectors to  $\Omega$ .

Let the boundary  $\partial\Omega$  be decomposed in two disjoint subsets  $\Gamma_D \neq \emptyset$  and  $\Gamma_N$ . The assumption on  $\Gamma_D$  (of nonzero Lebesgue measure) is necessary for the uniqueness of the solution. The model problem is given by the following strong form set of equations:

$$\begin{aligned} -\Delta_{\Omega} u &= f & \text{in } \Omega, \\ u &= u_D & \text{on } \Gamma_D, \\ \nabla_n u &= t_N & \text{on } \Gamma_N. \end{aligned} \quad (2)$$

where the operator  $\Delta_{\Omega}$  is defined as  $\nabla_{\Omega} \cdot \nabla_{\Omega}$  and  $\nabla_n u$  is the outward flux through the boundary  $\Gamma_N$  of  $\Omega$ . Notice that Dirichlet  $u_D$  and Neumann  $t_N$  boundary conditions are enforced on boundaries of at least one codimension higher than that of the domain.

Thus,  $\Gamma_D$  and  $\Gamma_N$  may be points for embedded 1D-submanifolds, lines for 2D-submanifolds or surface for the 3D case. Currently, imposing Dirichlet boundary conditions within the X-FEM has only been studied with embedded submanifolds of codimension zero. In this paper, we do not limit ourselves to these configurations and investigate any embedding as depicted in Figure 2.

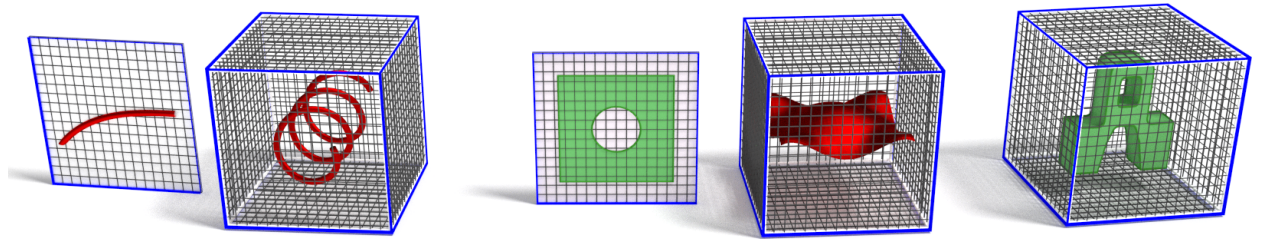


Figure 2: Embedded solids (from left to right) : 1D-submanifolds of codimension one or two, 2D-submanifolds of codimension zero or one, 3D-submanifold of codimension zero.

### 2.1. Weak formulations

Let us introduce the setting in order to derive the weak form of the one-field problem resulting from the above equations. Let  $\mathcal{U} := H^1(\Omega)$ , we seek solutions in the subset  $\mathcal{U}_D := \{u \in \mathcal{U} : u = u_D \text{ on } \Gamma_D\}$ , using test functions living in  $\mathcal{U}_0 := \{u \in \mathcal{U} : u = 0 \text{ on } \Gamma_D\}$ . The model problem given Equation (2) may be expressed as follows :

$$\text{Find } u \in \mathcal{U}_D : \int_{\Omega} \nabla_{\Omega} u \cdot \nabla_{\Omega} v \, d\Omega = \int_{\Omega} f v \, d\Omega + \int_{\Gamma_N} t_N v \, d\Gamma, \quad \forall v \in \mathcal{U}_0. \quad (3)$$

To remove the constraint on the primal field  $u$  defined here in  $\mathcal{U}_D$ , a two-field formulation may be constructed.

Considering  $u|_{\Gamma_D}$  defined in  $H^{1/2}(\Gamma_D)$  (the trace space of  $\mathcal{U}$  restricted to  $\Gamma_D$ ), we introduce  $\lambda$ , a Lagrange multiplier belonging to the dual space  $\mathcal{L} := (H^{1/2}(\Gamma_D))' = H^{-1/2}(\Gamma_D)$ . To enforce the Dirichlet BC on  $\Gamma_D$  (now a saddle-point problem), the associated weak formulation is :

Find  $(u, \lambda) \in \mathcal{U} \times \mathcal{L}$  :

$$\begin{aligned} \int_{\Omega} \nabla_{\Omega} u \cdot \nabla_{\Omega} v \, d\Omega - \int_{\Gamma_D} \lambda v|_{\Gamma_D} \, d\Gamma &= \int_{\Omega} f v \, d\Omega + \int_{\Gamma_N} t_N v \, d\Gamma, \quad \forall v \in \mathcal{U}; \\ - \int_{\Gamma_D} \mu u|_{\Gamma_D} \, d\Gamma &= - \int_{\Gamma_D} \mu u_D \, d\Gamma, \quad \forall \mu \in \mathcal{L}. \end{aligned} \quad (4)$$

Being in the framework of a mixed formulation, it is well established that the satisfaction of a discrete inf-sup conditions is required for interpolation spaces. In Sect. 3, the stability of this formulation will be preserved by carefully designing the Lagrange multipliers space, regardless of the codimension of the domain  $\Omega$ .

Instead of the previous technique using a dual space, the problem can be approximated by substituting the Dirichlet BC with a purely numerical forcing term in a Nitsche-type formulation. We briefly recall a symmetric version that will be used for comparison.

$$\begin{aligned} \text{Find } u \in \mathcal{U} : \quad & \int_{\Omega} \nabla_{\Omega} u \cdot \nabla_{\Omega} v \, d\Omega - \int_{\Gamma_D} \nabla_n u v \, d\Gamma - \int_{\Gamma_D} (u - u_D) \nabla_n v \, d\Gamma \\ & + \int_{\Gamma_D} \alpha (u - u_D) v \, d\Gamma = \int_{\Omega} f v \, d\Omega + \int_{\Gamma_N} t_N v \, d\Gamma, \quad \forall v \in \mathcal{U}. \end{aligned} \quad (5)$$

Here, the additional terms are respectively introduced (i) to provide consistency with regard to the boundary terms, (ii) to keep the symmetry of the equation and (iii) to ensure that it converges to the same solution as the initial problem, according to the parameter  $\alpha$ . More details on the choice of this parameter are given in Sect. 4 for numerical validation purpose.

## 2.2. Finite element discretisation

First of all, the geometry of the problem domain has to be approximated. The embedding is made into the ambient domain  $\mathcal{T}$  that is discretised quasi uniformly into shape-regular linear elements (lines in 1D, triangles in 2D or tetrahedra in 3D) of characteristic length  $h$ . The resulting mesh  $\mathcal{T}^h$  used for the field approximation is then independent of the geometry of the problem. Only the domain of integration  $\Omega^h$  must be adapted in order to be body-fitted, see Figure 3.

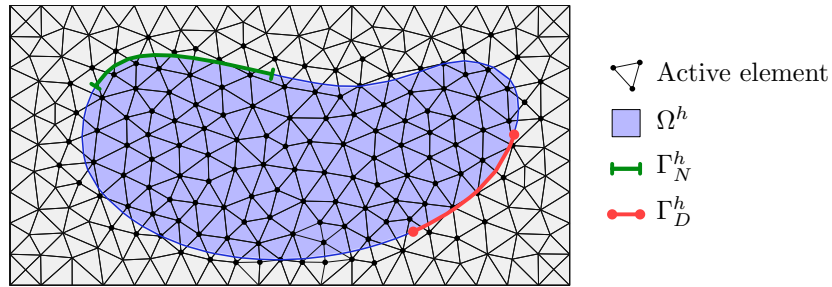


Figure 3: 2D model problem embedded in a bulk mesh  $\mathcal{T}^h$ . The discretised domain  $\Omega^h$  is subject to Dirichlet (resp. Neumann) type condition on the boundary  $\Gamma_D^h$  (resp.  $\Gamma_N^h$ ).

As mentioned above, an explicit or implicit geometric representation may be used within the X-FEM. It results in a linear approximation of the problem domain. Furthermore, the strategy to describe the geometry is combined with specific integration rules over embedded domains and boundaries involved in Equation (6). The level-set technique will be chosen in the numerical validations, with a regular Gauss quadrature used on sub-elements.

---

*Definition of the discrete function space*

The discretisation  $u^h$  of the bulk field is directly obtained if  $\text{codim}_{\mathcal{T}^h}(\Omega^h) = 0$ , using the function space  $\mathcal{U}^h \subset \mathcal{U}$  defined over the bulk mesh. In case of higher codimension,  $\Omega^h$  is not suitable for the definition of a finite element function space without remeshing (especially in 3D with a surface), therefore the traces of the shape functions defined on  $\mathcal{T}^h$  must be used. Analysis of the approximation properties of the linear trace spaces in codimension one is available in [68] for closed domains. Without boundaries, the enforcement of BCs on edges embedded in a 3D mesh is not addressed.

Nevertheless, the discretised problem becomes singular when the trace space is naively built using all the shape functions. Due to the fact that inner shape functions do not vanish on the boundary, it is not possible to directly use an L2-projection.

To illustrate it, we compare different spaces built from P1 Lagrange basis functions in Figure 4. The problem is defined on a straight line, and we check if it is well-posed thanks to the rank-nullity theorem. Starting with a P1-conforming space of polynomials of degree one on a 1D mesh, the non-conforming case is investigated with the embedding of the straight line in a 2D mesh. Considering the values at each intersecting points between the line and the elements as the unknowns, the rank of the full P1 trace space is always greater than the number of DOFs except if the boundary is conforming. The overdetermined system is reducible and some shape functions may be joined together, yielding a depleted function space. Specific treatments of the linear algebraic system of equations has been proposed in [69]. We choose an approach taking advantage of the fixed topology of the mesh introduced in [14]. The full P1 trace space may be reduced thanks to an algorithm — called vertex space reducer — which identifies the shape functions that are in excess and defines linear combinations for any codimension of the problem. This way, we extract a basis from the P1 space defined on  $\mathcal{T}^h$ . The resulting space is able to represent any linear field, for this reason it is called P1-equivalent. Of course, this approach leads to the classical finite element discretisation in case of a boundary fitted mesh. For the sake of conciseness, a unique notation for the discrete function space will be employed for any codimension of the problem.

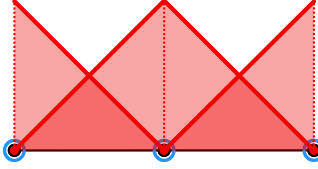
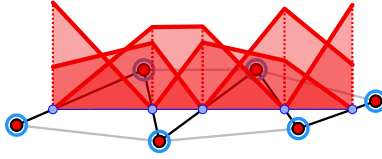
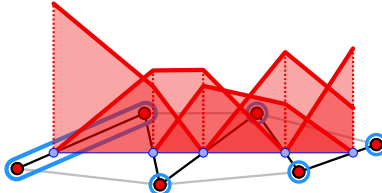
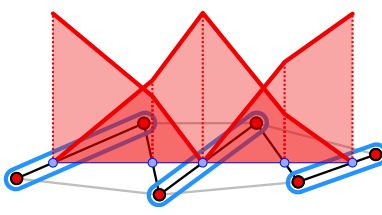
Space	Shape functions	number of DOFs	Rank
P1-conforming		3	3
Full P1		6	5
P1-equivalent		5	5
P0-equivalent		3	3

Figure 4: Comparison of various spaces built from the classical P1 Lagrange shape functions.

*Definition of the discrete Lagrange multiplier space*

By imposing the Dirichlet BCs in a two-field framework, the weak formulation given Equation (4) leads to the following discrete problem:

$$\begin{aligned}
 &\text{Find } (u^h, \lambda^h) \in \mathcal{U}^h \times \mathcal{L}^h : \\
 &\int_{\Omega^h} \nabla_{\Omega^h} u^h \cdot \nabla_{\Omega^h} v^h \, d\Omega - \int_{\Gamma_D^h} \lambda^h v^h|_{\Gamma_D^h} \, d\Gamma = \int_{\Omega^h} f v^h \, d\Omega + \int_{\Gamma_N^h} t_N v^h \, d\Gamma, \quad \forall v^h \in \mathcal{U}^h; \\
 &-\int_{\Gamma_D^h} \mu^h u^h|_{\Gamma_D^h} \, d\Gamma = -\int_{\Gamma_D^h} \mu^h u_D \, d\Gamma, \quad \forall \mu^h \in \mathcal{L}^h.
 \end{aligned} \tag{6}$$

Here, the discrete Lagrange multiplier space  $\mathcal{L}^h \subset \mathcal{L}$  is build on the FE approximation. A necessary condition to enforce weakly the Dirichlet BC on the primal field  $u^h$  (linearly approximated) is that any constant field must be reproduced by the Lagrange multiplier

space. A P1-equivalent space is indeed not required for the dual field. Furthermore, the inf-sup condition must be fulfilled by the duality pair of spaces  $\mathcal{U}^h$  and  $\mathcal{L}^h$ , as previously discussed. This condition ensures the uniqueness and the stability of the numerical solution and may be expressed as:

$$\exists c > 0, \forall h > 0 : \inf_{\lambda^h \in \mathcal{L}^h} \sup_{u^h \in \mathcal{U}^h} \frac{\int_{\Gamma_D^h} \lambda^h u^h|_{\Gamma_D^h} \, d\Gamma}{h^{1/2} \|\lambda^h\|_{L^2(\Gamma_D^h)} \|u^h\|_{H^1(\Omega^h)}} \geq c. \quad (7)$$

In line with the definition of the primal field, we adopt an approach based on mesh topology, leading to an *a priori* stable Lagrange multiplier space. It generalises the algorithm proposed in [48] to the wide class of embedded problems, with boundaries defined as submanifolds of codimension one or two in a 2D or 3D background mesh. Sect. 3 is devoted to detail the new approach. Starting with P1 Lagrange basis functions defined on the background mesh and used for the approximation of the dual field, linear combinations between their traces are introduced in order to recover a shape function density similar to the conforming case. We give, in Figure 4, an illustration of the resulting space, denoted P0-equivalent, on the previous 1D example. For approximatively the same characteristic length of the elements, between the meshes used with P1-conforming and P0-equivalent spaces, we highlights strong similarities between their shape functions.

In order to measure the stability of the resulting formulation, the numerical Chapelle-Bathe test — also called inf-sup test — has been proposed in [70, 71]. The solution of the following eigenvalue problem will be computed through convergence studies conducted Sect. 4:

$$\frac{1}{h} (B_h^T M_h^{-1} B_h) V_h = \beta_h A_h V_h. \quad (8)$$

Here,  $A_h$ ,  $B_h$  and  $M_h$  are respectively the energy matrix (on  $\Omega^h$ ), the coupling and the  $\lambda^h$ -mass matrices (on  $\Gamma_D^h$ );  $V_h$  being the vector of bulk unknowns. The square root of the first non-zero eigenvalue in  $\{\beta_h\}$  gives the inf-sup constant  $c$  associated with the discrete problem. In practice, this constant should be mesh-independent, otherwise the inf-sup condition is not satisfied. This test has already been considered in [18, 48] within similar frameworks.

### 3. Design of the stable Lagrange multiplier space

To address the imposition of Dirichlet BCs on embedded boundaries for any configuration of the model problem, some general concepts (available in 1D, 2D and 3D) will be introduced. They allow to extend stable Lagrange multiplier methods [18, 66, 48, 44] to 1D boundaries embedded in 3D (codimension two) in a single framework.

#### 3.1. Terminology

The proposed solution deeply uses the terminology introduced in [14]. We briefly recall the main ideas. We define the *supports* as the mesh components on which the embedded domain discretisation — made of sub-components — is built. In this way, we get access to the bulk shape functions of the mesh  $\mathcal{T}^h$  from the underlying discretisation of the embedded geometry  $\Omega^h$  (or  $\Gamma_D^h$  here), using the mesh topology. One only have to select supports properly to form a free basis of Lagrange multipliers defined on  $\Omega^h$ . This selection must satisfy the following conditions to be consistent with FEM.

**Definition 3.1.** *Vital support.* A vital support results in one Lagrange multiplier (a linear combination of the associated shape functions). Its define according to :

- (i) a condition on the conformity: a support which conforms to  $\Gamma_D^h$  is denoted vital,
- (ii) a condition on the linear independency: vital supports constitute disjoint sets,
- (iii) a condition on the partition of unity: shape functions of a non-vital support must be linked at least to one vital support.

Similar concepts have been introduced in [18, 66, 48], but only edges of the mesh were used to identify the shape functions. Furthermore, the non-uniqueness in the choice of the resulting Lagrange multiplier space was reported. The same applies with the graph of vital supports.

To this end, deterministic criteria will be introduced in the proposed algorithm accordingly to the following score.

**Definition 3.2.** *Support score.* Let  $\mathcal{S}$  be a support of dimension  $\leq \text{codim}_{\mathcal{T}^h}(\Gamma_D^h)$  on which a node of  $\Gamma_D^h$  (i.e. a 0D sub-component) is defined. We associate the number of supports of dimension  $\leq \text{codim}_{\mathcal{T}^h}(\Gamma_D^h)$  connected to  $\mathcal{S}$ .

We illustrate the computation of support scores on various configurations in Figure 5. The scores are written next to the nodes of  $\Gamma_D^h$  for a better visualisation.

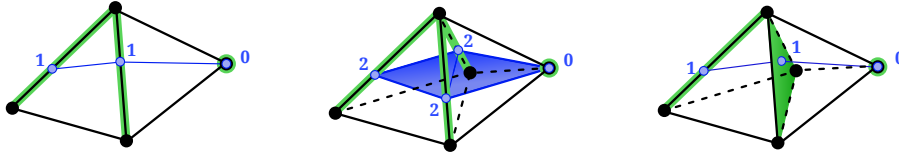


Figure 5: Support scores in two or three dimensions with embedded boundaries of codimension one (left, middle) or two (right).

Assuming that one Lagrange multiplier is defined at each support of dimension  $\leq \text{codim}_{\mathcal{T}^h}(\Gamma_D^h)$ , the support score allows to detect how many Lagrange multipliers would be depleted if we identify a support as vital. This corresponds to the number of connections in the support graph. The detailed steps of the selection procedure are given in the sequel.

### 3.2. Description of the algorithm

The design of a stable Lagrange multiplier space must be a compromise between two contradictory requirements. On the one hand, the number of shape functions must be reduced to satisfy the inf-sup condition and preclude instabilities. On the other hand, the space of Lagrange multipliers must be as large as possible in order to impose accurately the Dirichlet constraint.

Let us consider an embedded line  $\Gamma_D$  subjected to a Dirichlet boundary condition, with extremities being arbitrarily defined inside elements (Figure 6). In order to obtain a better approximation of the Lagrange multipliers and evaluate at the endpoints of the line the scores previously introduced, we extend the discretised domain  $\Gamma_D^h$  into a larger domain  $\overline{\Gamma_D^h}$ . This is achieved by using a linear extension in the elements containing the endpoints.

Figure 7 illustrates this first step, as well as the following in the algorithm producing a stable Lagrange multiplier space. Algorithm 1 details the pseudocode in an implementation perspective.

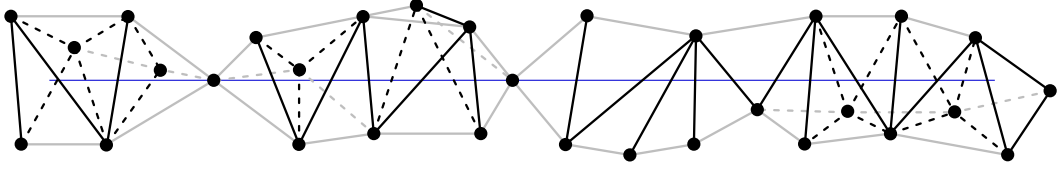
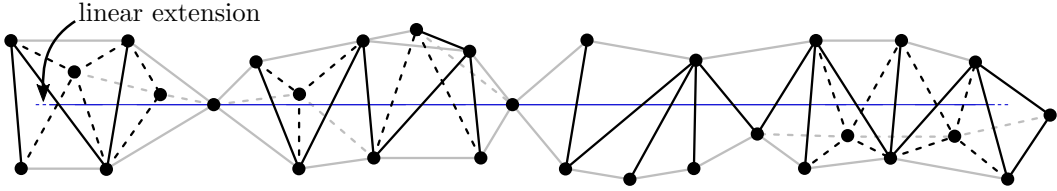
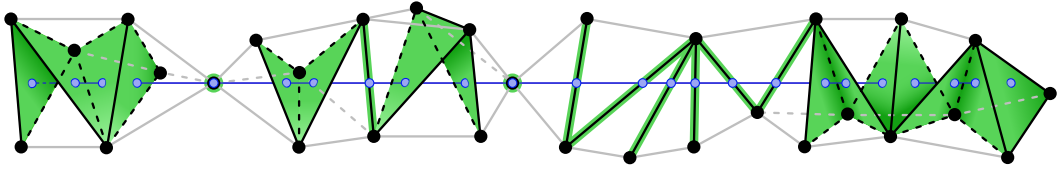


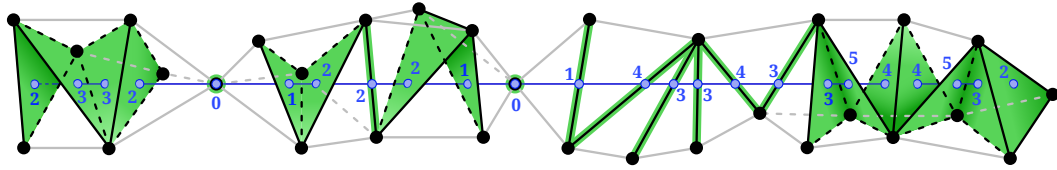
Figure 6: An embedded line that is unfitted to the narrow band of elements.



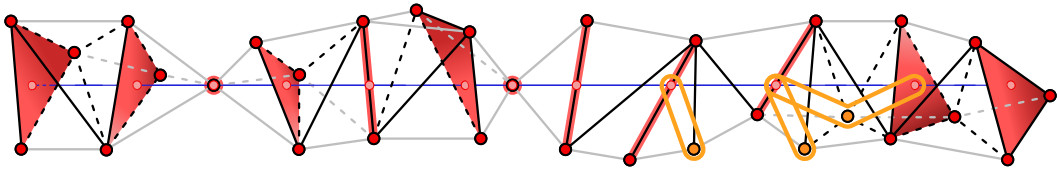
(a) Linear extension of the embedded line.



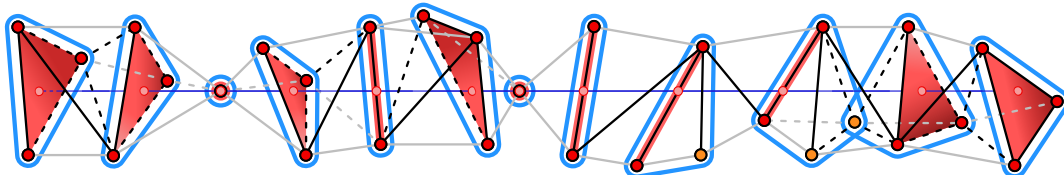
(b) Supports of the intersection points of the embedded line with the mesh.



(c) Vertex scores (*italic*) and support scores (**bold**) along the embedded line.



(d) `Full_Shape_Functions` (drawn in red) and `Distributed_Shape_Functions` (outlined in orange) associated with vital supports.



(e) Set of Lagrange multiplier shape functions.

Figure 7: The four steps of the algorithm and the final P0-equivalent space.

---

**Algorithm 1:** Vital support reducer.

---

**Input:** (Figure 6)

A boundary set  $\Gamma_D^h$  of elements or sub-elements embedded in a background mesh.

**Output:** Identification of vital supports.

Characterisation of the vertex shape functions: **Full\_Shape\_Function** (resp. **Distributed\_Shape\_Function**) associated with its unique vital support (resp. distributed on the vital supports which are connected to the vertex through its connected supports of dimension  $< \text{codim}_{\mathcal{T}^h}(\Gamma_D^h)$ ).

1: (Figure 7a)

**if**  $\partial\Omega \neq \emptyset$  **then**

    | Build  $\overline{\Omega^h}$  the linear extension of  $\Omega^h$ ,

**else**

    | Define  $\overline{\Omega^h} := \Omega^h$ .

2: (Figure 7b)

Build connectivities and supports of the group  $\Gamma_D^h$ .

3: (Figure 7c)

Compute scores of vertices and supports.

4: (Figure 7d)

Flag every supports of dimension zero as being **vital**.

Sort the other supports of dimension  $< \text{codim}_{\mathcal{T}^h}(\Gamma_D^h)$  by increasing scores in a set.

Supports with the same score should be ordered in a deterministic way (e.g. using a unique key obtained from those vertices).

**for each** support  $\mathcal{S}$  *in this set* **do**

**if**  $\mathcal{S}$  *has no flag* **then**

**for each** vertex  $v \in \mathcal{S}$  **do**

            |  $v$  is flagged as **Full\_Shape\_Function**

            | Flag every support of dimension  $< \text{codim}_{\mathcal{T}^h}(\Gamma_D^h)$  and connected to  $v$  as

            | **non\_vital**.

        |  $\mathcal{S}$  is flagged as **vital**.

**for each** vertex  $v$  *connected to the boundary* **do**

**if**  $v$  *has no flag* **then**

        |  $v$  is flagged as **Distributed\_Shape\_Function**

---

Note that, in the case of a boundary of codimension one, the resulting Lagrange multiplier space exactly matches the one obtained through the procedure introduced in [48]. Consequently, the mathematical proof (in 2D) of a uniform inf-sup given in that paper holds in our setting. Furthermore, its validity is independent of how the `Distributed_Shape_Functions` are distributed over vital supports. The partition of unity may be satisfied locally, as proposed by Hautefeuille *et al.* [44], with a uniform distribution over Lagrange multipliers at the element level (the resulting shape functions are only piecewise  $C_0$ -continuous, with potentially inter-element discontinuities). In line with [48], we arbitrarily choose to enforce the partition of unity globally, using a single distribution independent of the element, in order to build  $C_0$ -continuous shape functions. This distribution is considered uniform over associated vital supports in the numerical applications presented next. Any other choice satisfying the partition of the unity is still valid, e.g. shape functions weighted according to the relative distance between the associated vertex and intersection points of vital supports with  $\overline{\Omega^h}$ . Further investigations on the numerical stability of these alternatives would be of interest in the perspective of solving problems with moving interfaces.

#### 4. Numerical validations

In this section, we present some numerical results illustrating how the proposed approach is suitably efficient and versatile. Boundary value problems involving a Dirichlet constraint on a boundary of dimension one (a line in 2D and 3D), and of dimension two (a surface in 3D) are solved. Due to the simplicity of imposing a boundary condition on an embedded point in 1D, 2D and 3D — by using a linear combination or a Lagrange multiplier — these trivial cases will not be included in the numerical tests. Convergence studies are performed on non-matching meshes and classical FE counterparts. We check numerically the compatibility between the primal field and the dual field of Lagrange multipliers by means of inf-sup tests. The accuracy of the results is compared with those obtained by Nitsche's method, when an analytical expression of the associated parameter is available at the element level.

We summarised in the sequel some implementation details used through the numerical validations.

#### *Selection of Nitsche's parameter*

Nitsche's formulation given in Equation (5) is discretised as follows:

Find  $u^h \in \mathcal{U}^h$  :

$$\begin{aligned} \int_{\Omega^h} \nabla_{\Omega^h} u^h \cdot \nabla_{\Omega^h} v^h \, d\Omega - \int_{\Gamma_D^h} \nabla_n u^h v^h \, d\Gamma - \int_{\Gamma_D^h} (u^h - u_D) \nabla_n v^h \, d\Gamma \\ + \int_{\Gamma_D^h} \alpha (u^h - u_D) v^h \, d\Gamma = \int_{\Omega^h} f v^h \, d\Omega + \int_{\Gamma_N^h} t_N v^h \, d\Gamma, \quad \forall v^h \in \mathcal{U}^h. \end{aligned} \quad (9)$$

Here, the parameter  $\alpha$  dictates the performance of the resulting formulation. Its choice must be a compromise between: (i) a sufficiently large value to ensure the coercivity of the formulation, and (ii) a reasonable small value to preserve good matrix conditioning of the problem.

Instead of a unique parameter defined over the whole boundary  $\Gamma_D^h$  as in [57], we choose a local definition introduced in [45] and used in [44]. We just recall the analytical expression that will be exploited in the numerical validations, and refer the interested reader to the mentioned references for more details. In each element  $e \in \mathcal{T}^h$  crossed by  $\Gamma_D^h$ , we consider a local parameter given by the analytical expression:

$$\alpha_e := 2 \frac{\text{meas}(\Gamma_D^h \cap e)}{\text{meas}(\Omega^h \cap e)}. \quad (10)$$

#### *Flux approximation using a domain integral post-processing technique*

Several ways may be investigated in order to evaluate the interfacial flux. In a mixed formulation, the fluxes can be represented as unknowns of the system, by using the Lagrange multipliers introduced for the BCs enforcement for instance. In other cases, the normal gradient operator may be simply applied on the bulk solution along the boundary. Unfortunately, this approach results in a poor evaluation of the interfacial flux. A flux projection operator introduced in the Domain Integral (DI) method [47] is a good alternative for this purpose. Using the P1 Lagrange shape functions  $N_i$  defined on the bulk mesh, we approximate the

interfacial flux at the vicinity of the interface by interpolating the nodal field defined as:

$$DI(\nabla_n u)_i := \frac{1}{\int_{\Gamma_D^h} N_i \, d\Gamma} \sum_e \int_{\Omega^h \cap e} \nabla N_i \nabla u^h - N_i f \, d\Gamma. \quad (11)$$

#### *Conditioning of the linear system*

Some consideration about ill-conditioning caused by small intersections of the domain with the mesh have to be given. In line with the previous paper [14], we consider the approach modifying the geometry to address conditioning issues of the resulting linear system, in a preliminary step to the Algorithm 1. In such a way,  $\Omega^h$  is locally modified into  $\widetilde{\Omega}^h$  before constructing the linear extension  $\widetilde{\widetilde{\Omega}^h}$ . Of course, an alternative approach modifying the function space may also be suitable, as long as the resulting P1 space defined over  $\widetilde{\widetilde{\Omega}^h}$  preserves a certain accuracy of the approximation (see [14]).

#### *4.1. Dirichlet constraints on an embedded line in 2D*

Imposing Dirichlet BCs using a stable Lagrange multiplier space in 2D has already been discussed in the literature, with convergence studies and a proof of stability [48]. Despite that, this validation aims to:

- (i) check that our approach is conservative within this setting,
- (ii) compare its accuracy with Nitsche's method in a convergence study.

We perform a 2D-numerical test proposed in [63], with a star-shaped curved boundary defined as the iso-zero of the distance function:

$$\psi(x, y) = -5 \left( 0.47^4 - \rho^4 [2.5 + 1.5 \sin(8\theta + 2\pi/9)] \right), \quad (12)$$

where  $(\rho, \theta)$  are the polar coordinates associated with  $(x, y)$ .

The strong form set of equations is given as follows:

$$\begin{aligned} -\Delta_\Omega u &= 0 & \text{in } \Omega &:= \{(x, y) \in \mathbb{R}^2 : \psi(x, y) < 0\}, \\ u &= u_D & \text{on } \Gamma_D &:= \{(x, y) \in \partial\Omega : y < 0\}, \\ \nabla_n u &= t_N & \text{on } \Gamma_N &:= \partial\Omega \setminus \overline{\Gamma_D}. \end{aligned} \quad (13)$$

Here, the Dirichlet  $u_D$  and Neumann  $t_N$  boundary conditions are defined thanks to the exact solution of this 2D Laplace problem given by  $u(x, y) = \psi(x, y)$ .

Illustrations of the first discretisation used in a convergence study and the exact solution are shown in Figure 8.

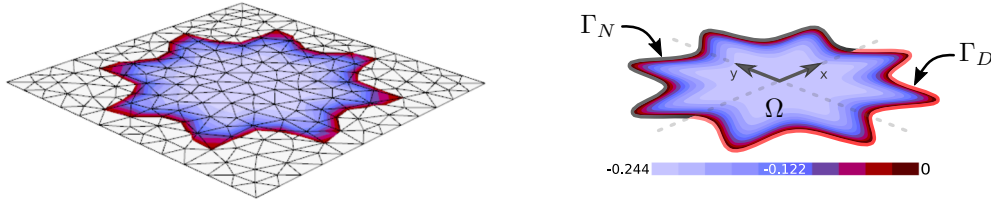


Figure 8: Geometry of the computational domain and exact solution of the star-shaped Laplace problem with an embedded line as Dirichlet boundary.

We perform a comparative study between three different approaches imposing the Dirichlet boundary condition:

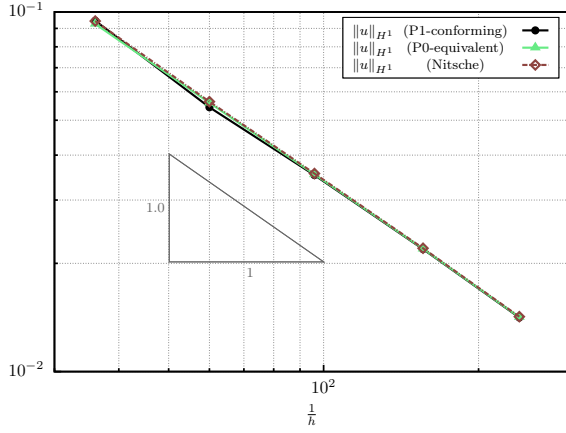
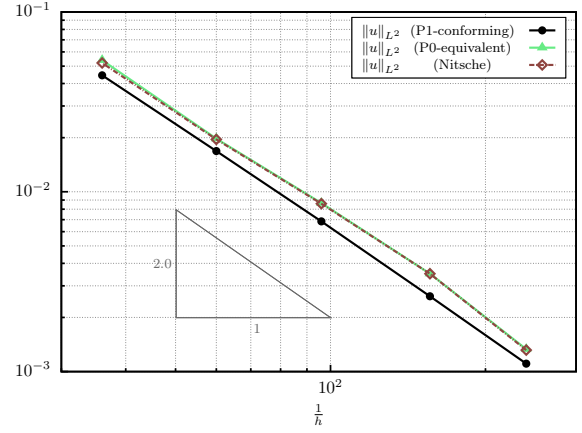
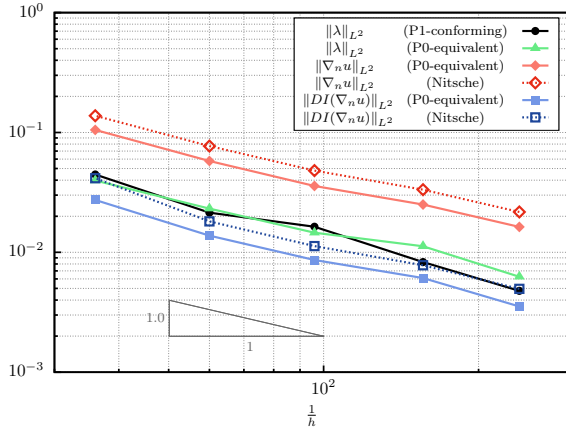
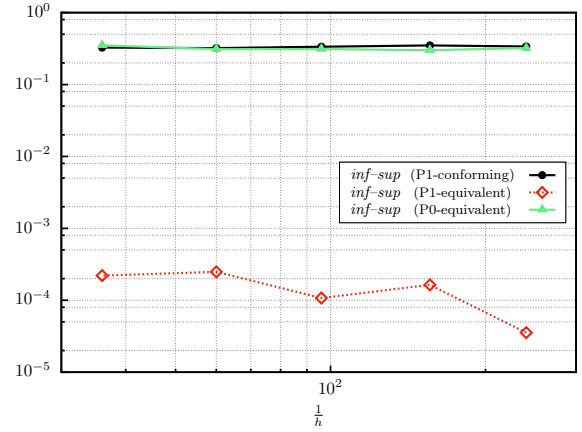
- by using Lagrange multipliers defined on P1-conforming elements as reference,
- by constructing a stable Lagrange multiplier space introduced in this paper as a P0-equivalent space,
- or by means of Nitsche's method.

For the two latter approaches based on non-conforming meshes, several ways to calculate the normal flux along the interface  $\Gamma_D$  are considered. Each one's notation is given in Table 1, followed by its description.

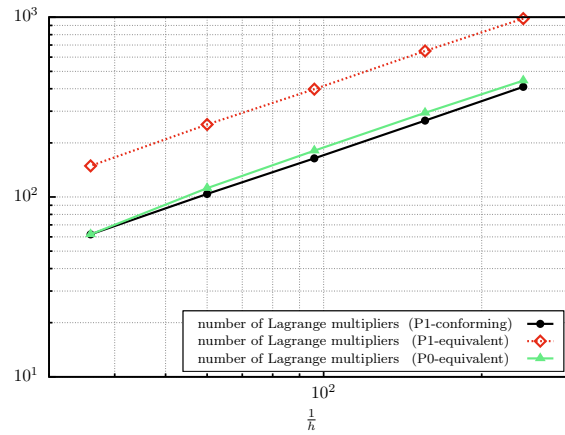
Table 1: Three different ways to evaluate the flux, with associated notations.

Notation	Description
$\lambda$	The flux is already calculated via the Lagrange multipliers.
$\nabla_n u$	The flux is obtained directly from the gradient of the solution.
$DI(\nabla_n u)$	The flux is post-treated using the domain integral method.

Figure 9 shows the results of convergence obtained on a sequence of meshes with increasing (uniform) density.


 (a) Error in the  $H^1$ -norm on the bulk field.

 (b) Error in the  $L^2$ -norm on the bulk field.

 (c) Error in the  $L^2$ -norm on the interfacial flux.


(d) Value of the inf-sup parameter.



(e) Number of Lagrange multipliers.

Figure 9: Convergence study for the Laplace problem solved on a star-shaped domain of codimension zero, with a Dirichlet condition defined on a boundary of codimension one.

The errors in the  $H^1$ - and  $L^2$ -norms decay optimally with all procedures as shown in Figures 9a and 9b. Figure 9c presents the error in the  $L^2$ -norm on the interfacial flux. The direct estimation of the normal flux gives a less accurate result for both non-conforming methods. The proposed approach gives comparable results with the conforming case (also using Lagrange multipliers). A better approximation of the flux is achieved with domain integrals, and the results obtained with the P0-equivalent space show the smallest error. P0-equivalent and P1-conforming spaces lead to similar inf-sup constants, see Figure 9d, whereas the naive choice of a P1-equivalent space introduced in [14] does not satisfy the inf-sup condition. An analysis of Figure 9e highlights a prohibitive number of Lagrange multipliers induced by this space with respect to the classical FEM. The P0-equivalent space allows to reduce this density to be similar to the P1-conforming one.

#### 4.2. Dirichlet constraints on an embedded line in 3D

We now consider configurations of the model problem with a Dirichlet constraint enforced on a boundary of codimension two in 3D. This setting has not yet been investigated on non-conforming meshes in the literature (but only on boundary-fitted meshes, e.g. in [72]), thereby no expression of the stability parameter is available for Nitsche's method. For this reason, comparative studies will be exempted from this method.

##### 4.2.1. Unit-square of codimension one

Let us start solving a unit-square Laplace problem of codimension one defined over an embedded flat surface in a 3D bulk mesh. It has already been considered in a previous paper [14] with 1D boundaries fitted with faces of the discretisation. In the sequel, the geometry is strictly included in the ambient mesh and the boundaries may cross the elements. The problem is posed as follows:

$$\begin{aligned} -\Delta_{\Omega} u &= 0 & \text{in } \Omega &:= ]0, 1[ \times ]0, 1[ \times \{0\}, \\ u &= u_D & \text{on } \Gamma_D &:= \{0\} \times ]0, 1[ \times \{0\}, \\ \nabla_n u &= t_N & \text{on } \Gamma_N &:= \partial\Omega \setminus \overline{\Gamma_D}. \end{aligned} \tag{14}$$

The boundary conditions are enforced according to the analytical solution given in the 3D Cartesian coordinates by :

$$u(x, y, z) = [\cosh(\pi x) - \coth(\pi) \sinh(\pi x)] \sin(\pi y). \quad (15)$$

The geometry of the domain within a non-matching unstructured mesh of tetrahedral elements and the bulk solution are illustrated in Figure 10.

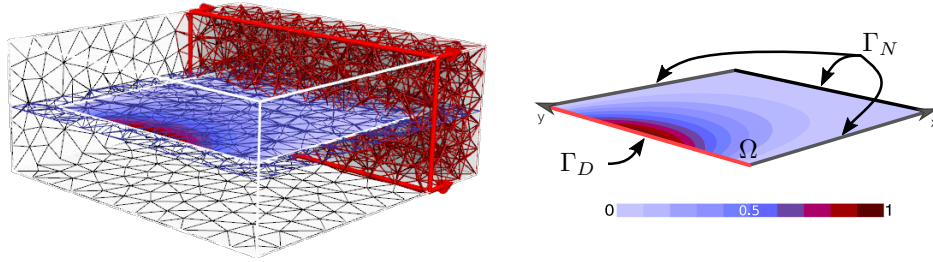
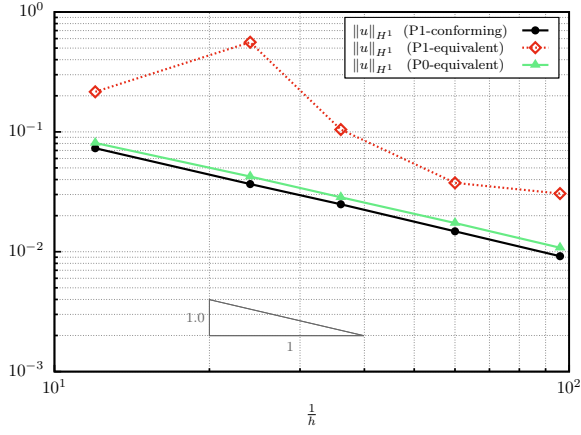
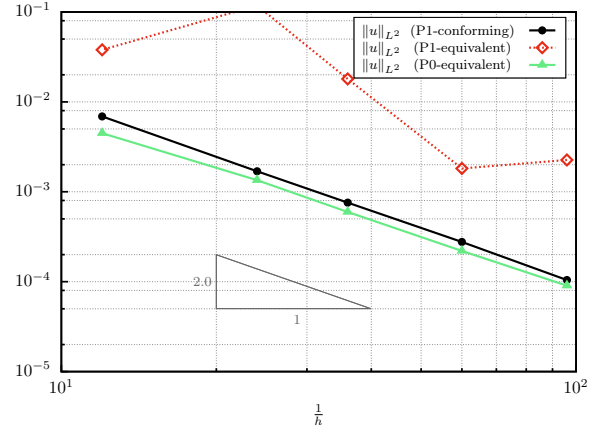
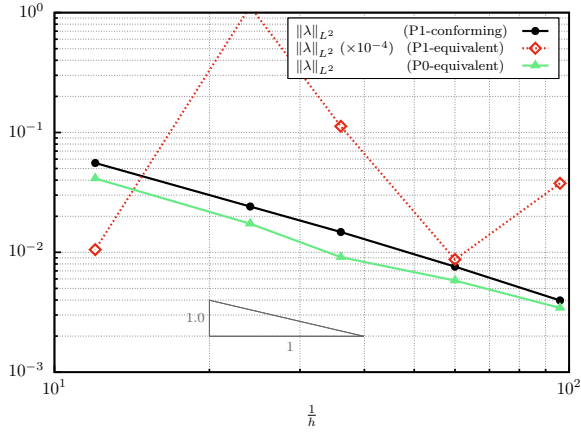
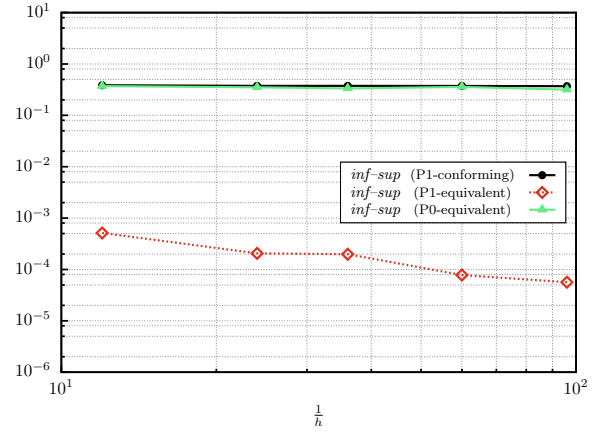


Figure 10: Geometry of the computational domain and exact solution of the unit-square Laplace problem with an embedded line as Dirichlet boundary.

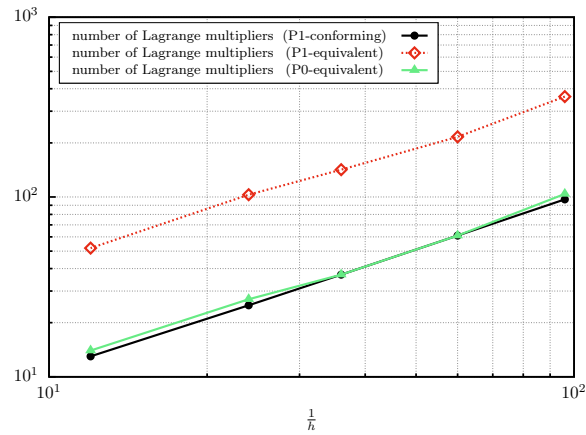
Using the FEM on a boundary-fitted mesh as a reference, we investigate the non-conforming case with two different Lagrange multiplier spaces:

- a P1-equivalent space of Lagrange multipliers, dedicated to model linear fields as proposed in [14],
- a P0-equivalent space, newly introduced in this paper, defining Lagrange shape functions on vital supports along the embedded line in 3D.

The results of a convergence study are given in Figure 11.


 (a) Error in the  $H^1$ -norm on the bulk field.

 (b) Error in the  $L^2$ -norm on the bulk field.

 (c) Error in the  $L^2$ -norm on the interfacial flux.


(d) Value of the inf-sup parameter.



(e) Number of Lagrange multipliers.

Figure 11: Convergence study for the Laplace problem solved on a unit-square of codimension one, with a Dirichlet condition defined on a boundary of codimension two.

Figures 11a and 11b show the errors in the  $H^1$ - and  $L^2$ -norms on the bulk field as a function of the mesh size  $h$ . As expected, the results obtained with the P1-equivalent space of Lagrange multipliers do not converge at all, with very high error in the  $L^2$ -norm on the interfacial flux as reported in Figure 11c. This choice fails due to locking that occurs as shown in Figure 11d with a non-uniform inf-sup estimate. The errors for the P0-equivalent space decay optimally when compared to a P1-conforming mesh. Furthermore, this new Lagrange multiplier space is stable and passes the numerical patch test on boundaries of codimension two. The relevant number of DOFs involved is then equivalent to the P1-conforming space, which is far from being the case with the P1-equivalent space.

Although the geometry presented here is straight, we contend that the proposed approach behaves analogously with a curved boundary which is linearly approximated, since it is based solely on the topology of the mesh.

#### 4.2.2. Unit-cube of codimension zero

The enforcement of boundary conditions on a point in 2D, on a point in 3D and on an edge in 3D, is in practice frequently used by engineers in FE packages. However, these are borderline cases where the associated problems may be singular. Indeed, the physical problem corresponding to the model depends on the size of the elements. This amounts to distribute the loadings on the elements that are around the point or the edge.

In order to present a convergence study for which theoretical convergence rates in the errors in  $H^1$  and  $L^2$ -norms may be achieved, we choose a case involving a smooth analytical solution with no singularity. It will be sufficient to show that the FE space built upon the background mesh must be reduced.

We consider the following Laplace problem of codimension zero defined on a unit-cube embedded in a bulk mesh:

$$\begin{aligned} -\Delta_{\Omega} u &= 0 & \text{in } \Omega &:= ]0, 1[ \times ]0, 1[ \times ]0, 1[, \\ u &= u_D & \text{on } \Gamma_D &:= \{0\} \times \{0\} \times ]0, 1[, \\ \nabla_n u &= t_N & \text{on } \Gamma_N &:= \partial\Omega \setminus \overline{\Gamma_D}. \end{aligned} \tag{16}$$

We define the boundary conditions in such a way as to satisfy the following analytical solution:

$$u(x, y, z) = [\cosh(\pi x) - \coth(\pi) \sinh(\pi x)] [\cosh(\pi y) - \coth(\pi) \sinh(\pi y)] \sin(\sqrt{2}\pi z). \quad (17)$$

Figure 12 shows the embedding of the domain problem in an unstructured mesh and the bulk solution.

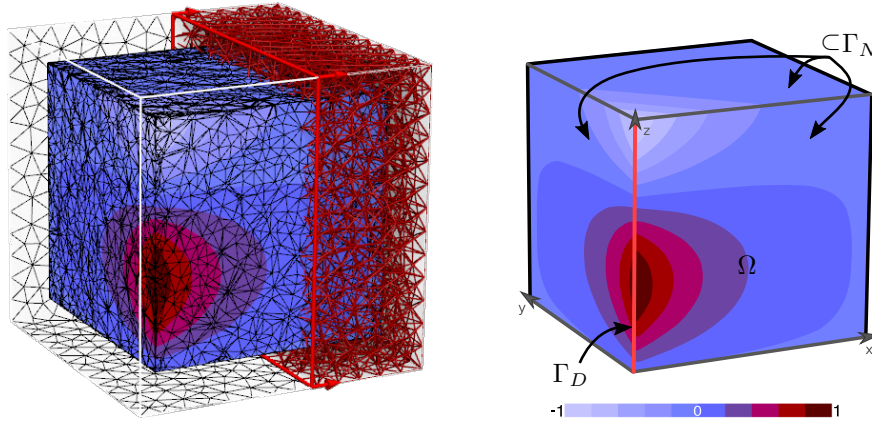


Figure 12: Geometry of the computational domain and exact solution of the unit-cube Laplace problem with an embedded line as Dirichlet boundary.

A convergence study is performed for the three approaches previously introduced (P1-conforming, P1-equivalent and P0-equivalent). The results are given in Figure 13.

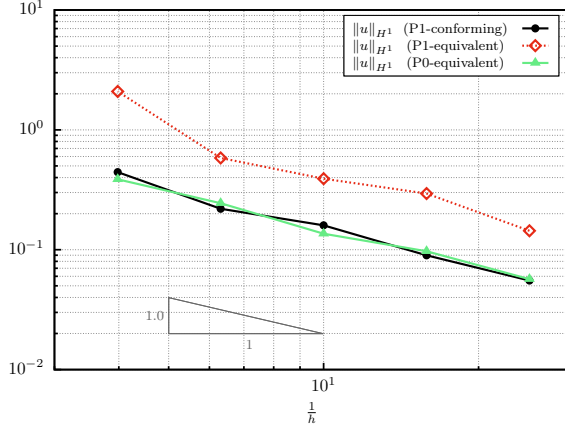
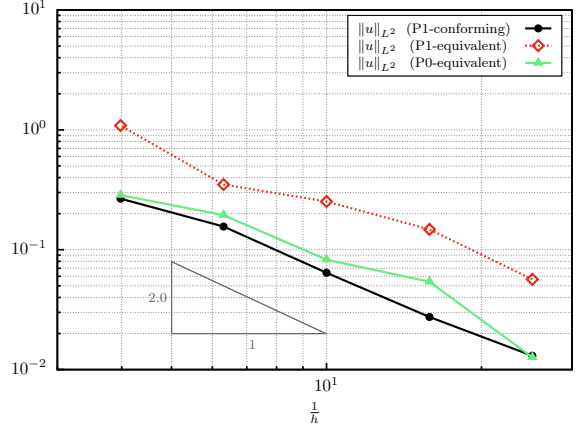
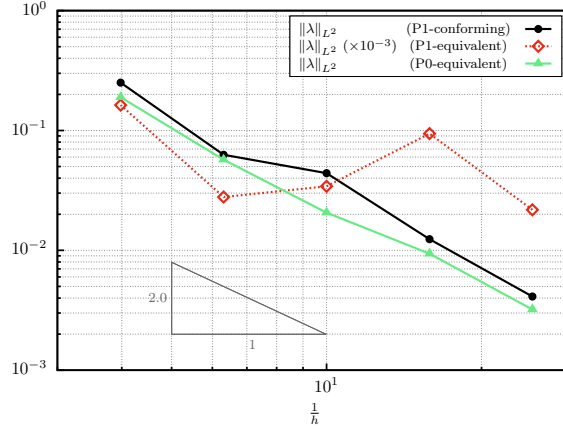
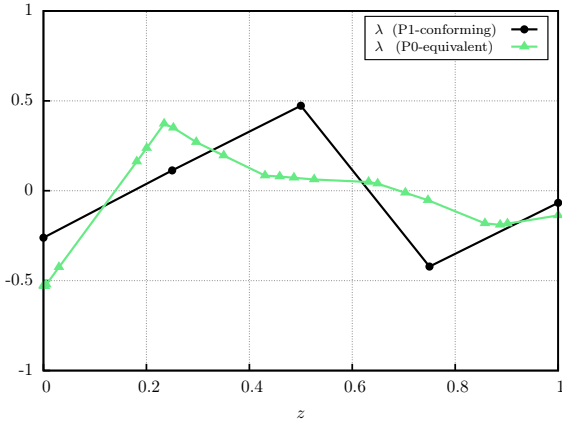
(a) Error in the  $H^1$ -norm on the bulk field.(b) Error in the  $L^2$ -norm on the bulk field.(c) Error in the  $L^2$ -norm on the interfacial flux.

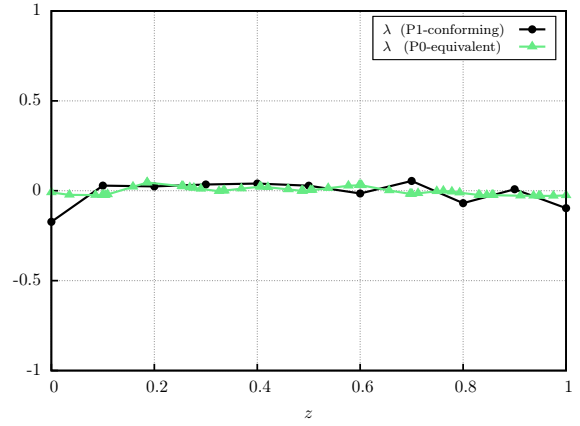
Figure 13: Convergence study for the Laplace problem solved on a unit-cube of codimension zero, with a Dirichlet condition defined on a boundary of codimension two.

The errors on the bulk field in the  $H^1$ - and  $L^2$ -norms are shown in Figures 13a–13b. A similar behaviour of the P1-conforming approach and the one using P0-equivalent space is observed. As depicted in Figure 13c, Lagrange multipliers are as good for both cases, whereas the approach based on the P1-equivalent space does not converge. Unlike previous cases, the existence of an inf-sup condition has not been treated in the literature when a gap of two dimensions appears between  $\Gamma_D$  and the domain  $\Omega$ , the theoretical developments being limited to the codimension one, see [73].

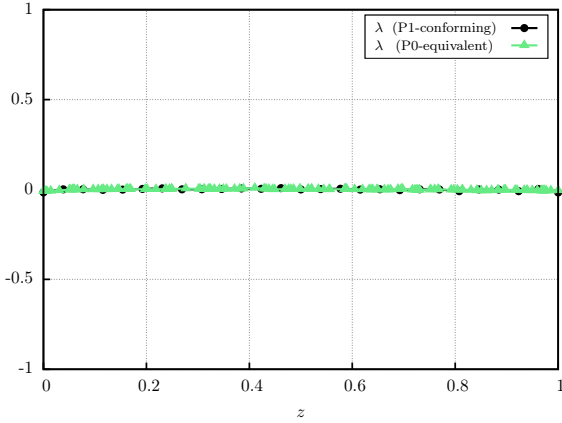
However, Lagrange multipliers must tend to zero through mesh refinement without spurious oscillations, since the constraint forces to impose Dirichlet condition are spread over the neighbouring elements of the edge whose size decreases. To check that, the distribution of the Lagrange multipliers along the edge is shown in Figure 14 for a sequence of unstructured meshes (the first, third and fifth mesh of the convergence study).



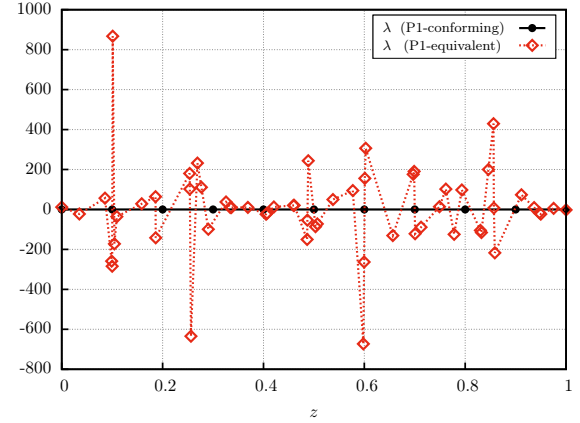
(a) Lagrange multipliers obtained with  $\frac{1}{h} = 4$ .



(b) Lagrange multipliers obtained with  $\frac{1}{h} = 10$ .



(c) Lagrange multipliers obtained with  $\frac{1}{h} = 25$ .



(d) Lagrange multipliers obtained with  $\frac{1}{h} = 10$ .

Figure 14: Distribution of the Lagrange multipliers for the Laplace problem solved on a unit-cube of codimension zero, with a Dirichlet condition defined on a boundary of codimension two.

Results obtained with our new stable Lagrange multiplier space and with a boundary-

fitted approach are compared in Figures 14a–14c. They show that moderate oscillations obtained with the coarsest meshes vanish with the increase of the mesh density. This is not the case with the P1-equivalent space, for which ubiquitous oscillations appear with strong magnitudes as depicted in Figure 14d.

#### 4.3. Dirichlet constraints on an embedded surface in 3D

Let us now examine the case of embedded solids of codimension zero in 3D. To enforce the Dirichlet constraints, a comparison is made between four different methods. Three are based on Lagrange multipliers:

- The first introduces Lagrange multipliers on a boundary-fitted mesh,
- The second is the one presented here, noted P0-equivalent and building continuous shape functions, ensuring the partition of unity at global level over the entire interface.
- The third, denoted P0\*-equivalent, was introduced in [44] and defines piecewise continuous shape functions, only locally ensuring the partition of unity.

Finally, the fourth approach uses Nitsche’s method.

- It corresponds to the method used in [44].

As previously introduced in Sect. 4.1, the interfacial flux through embedded boundaries is evaluate using different ways (direct evaluation, Lagrange multipliers, or domain integrals), cf. Table 1.

By means of several three-dimensional benchmark problems, the relative performances of the P0\*-equivalent stable Lagrange multiplier method and of Nitsche’s method are investigated by Hautefeuille *et al.* in [44]. Based on their results and following discussions with the authors, some missteps in the mesh generation process make an analysis of the results very difficult (flat elements, negative jacobian). They drastically affect the accuracy of the results obtained with an approach based on mesh topology as is the case for stable Lagrange multiplier spaces. So the primary motivations of this part is to correct these results and to compare them with

solutions obtained with the P0-equivalent space designed through the new reducer algorithm. We also check numerically that both P0- and P0\*-equivalent approaches satisfy a uniform inf-sup condition.

Considering unstructured meshes defined over  $\mathcal{T} := ]0, 1[ \times ]0, 1[ \times ]0, 1[$ , two problems are presented. For each of them, an embedded surface  $\Gamma$  of different geometric shape is introduced in the bulk mesh, dividing the latter into two disjoint sets. The problem domain  $\Omega$  is then defined on one of these sets of codimension zero. We systematically analyse the approximations of the bulk and interfacial fields by means of convergence studies.

#### 4.3.1. Sinusoidal field with a Dirichlet constraint on an embedded planar surface

We first consider an embedded planar surface  $\Gamma$  defined as the iso-zero of the distance function  $\psi(x, y, z) = 0.2x - 0.2y + z - 0.4856$ . The boundary value problem consists in the following Poisson equation:

$$\begin{aligned} -\Delta_{\Omega} u &= -3\pi^2 \cos(\pi x) \cos(\pi y) \cos(\pi z) & \text{in } \Omega := \{(x, y, z) \in \mathcal{T} : \psi(x, y, z) > 0\}, \\ u &= \cos(\pi x) \cos(\pi y) \cos(\pi z) & \text{on } \Gamma_D := \Gamma \cup \{(x, y, z) \in \partial\Omega : z = 1\}, \\ \nabla_n u &= 0 & \text{on } \Gamma_N := \partial\Omega \setminus \overline{\Gamma_D}. \end{aligned} \quad (18)$$

The problem has an analytical solution given by  $u(x, y, z) = \cos(\pi x) \cos(\pi y) \cos(\pi z)$ . The boundary conditions are defined according to this expression. The embedded Dirichlet BC is limited to  $\Gamma$ , other parts being subject to constraints enforced in classical FE way. We illustrate the first unstructured mesh with the embedding of the manifold  $\Omega$  used in this study and the exact solution of the problem in Figure 15.

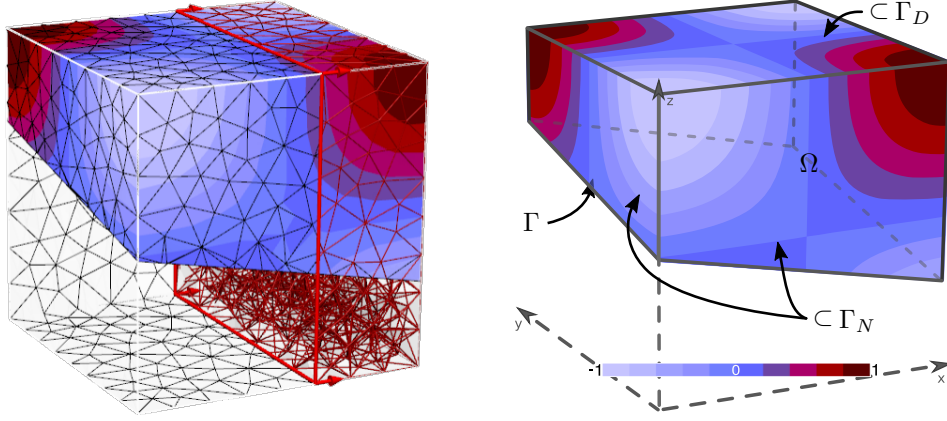
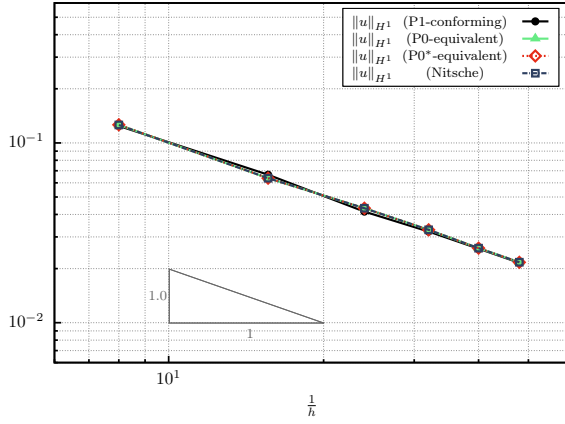
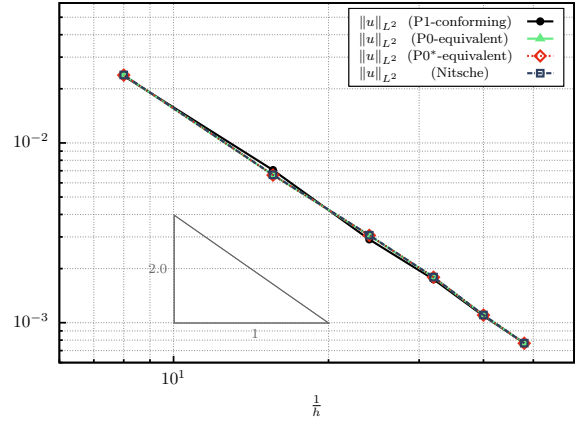
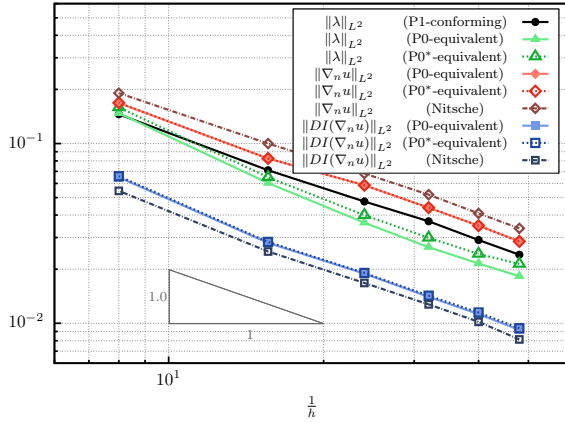
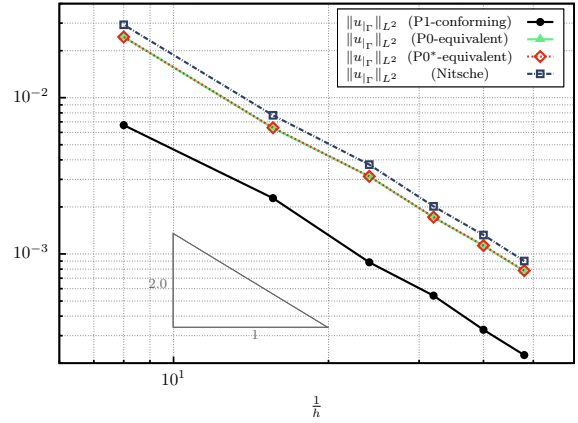
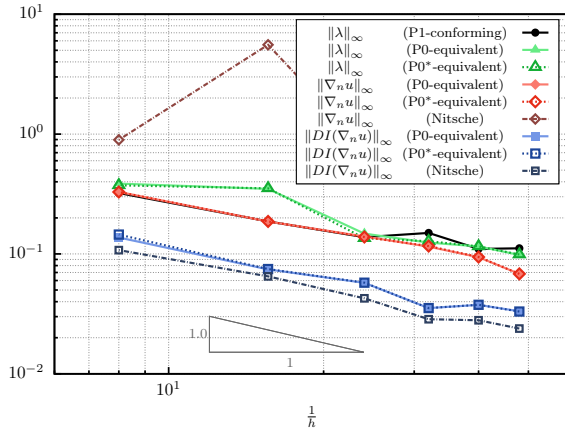
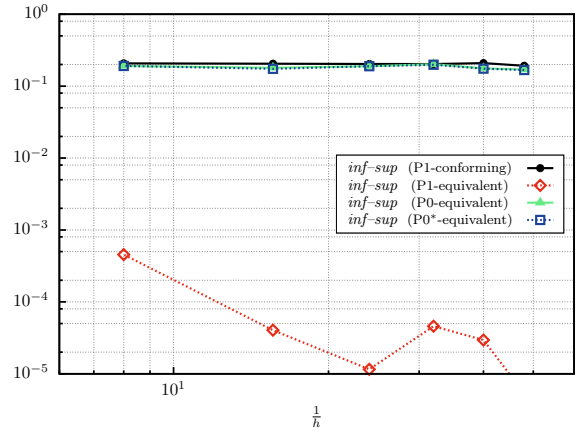


Figure 15: Geometry of the computational domain and exact solution of the Poisson problem, with an embedded planar surface as Dirichlet boundary.

The results of convergence are given in Figure 16.


 (a) Error in the  $H^1$ -norm on the bulk field.

 (b) Error in the  $L^2$ -norm on the bulk field.

 (c) Error in the  $L^2$ -norm on the interfacial flux.

 (d) Error in the  $L^2$ -norm on the interfacial field.

 (e) Error in the  $L_\infty$  norm on the interfacial flux.


(f) Value of the inf-sup parameter.

Figure 16: Convergence study for the Poisson problem with a Dirichlet boundary condition defined on an embedded planar surface.

Figures 16a and 16b show the optimal rate of convergence achieved with all procedures, in the  $H^1$ - and  $L^2$ -norms on the bulk field. The convergence results for the  $L^2$ -norm are given in Figures 16c and 16d, respectively on the flux and the field over the boundary  $\Gamma$ . The approximation of the normal flux is optimal. But as it might be expected, using the direct evaluation of the flux yields a much lower accuracy. Lagrange multipliers obtained with the  $P0^*$ -equivalent space proposed by Hautefeuille *et al.* are less accurate than ours, discontinuous bases being suspected to deteriorate the solution. The accuracy of the constraint enforcement is slightly better with Lagrange multipliers, cf. Figure 16d. In addition, Figure 16e presents the results in the sup-norm for the interfacial flux. We note that the maximum nodal error on the flux obtained directly with Nitsche's method does not converge. This poor result is due to the lack of robustness when the flux is estimated in elements with a very small intersection with the surface. The use of domain integrals over the three non-conforming approaches significantly improved the interfacial flux. As shown in Figure 16f, the inf-sup condition is violated by the P1-equivalent space, but the other Lagrange multipliers spaces are stable. These results are in good agreement with the number of Lagrange multipliers given in Figure 17, both  $P0$ - and  $P0^*$ -equivalent spaces acting as classical FEs.

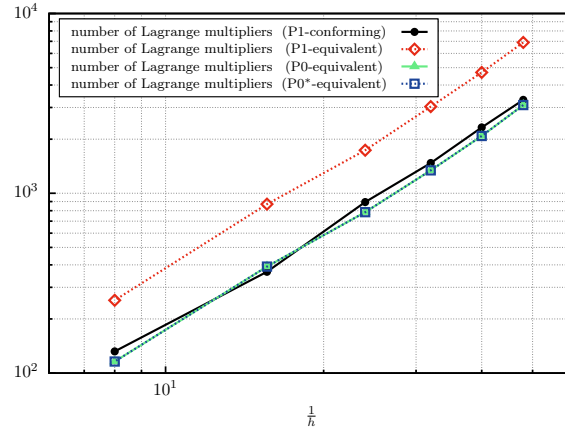


Figure 17: Number of Lagrange multipliers involved in the convergence study.

#### 4.3.2. Logarithmic field with a Dirichlet constraint on an embedded spherical surface

We now examine a Poisson problem involving an embedded spherical boundary. The governing equations and the boundary conditions are detailed below:

$$\begin{aligned} -\Delta_{\Omega} u &= -1/r^2 & \text{in } \Omega &:= \{(r, \theta, \varphi) \in \mathcal{T} : \psi(r, \theta, \varphi) > 0\}, \\ u &= \log r & \text{on } \Gamma_D &:= \Gamma \cup \{(x, y, z) \in \partial\Omega : \|(x, y, z)\|_{\infty} = 1\}, \\ \nabla_n u &= 0 & \text{on } \Gamma_N &:= \partial\Omega \setminus \overline{\Gamma_D}. \end{aligned} \quad (19)$$

Here,  $\|\cdot\|_{\infty}$  is the classical infinity norm defined on  $\mathbb{R}^3$ , its iso-values delimit a cubic domain. The iso-zero of the distance function  $\psi(r, \theta, \varphi) = r - 0.41$  defines the embedded Dirichlet boundary  $\Gamma$ , but only one-eighth of a sphere is modelled, thanks to the spherical symmetry of the problem about the origin. The analytical solution is known to be  $u(r, \theta, \varphi) = \log r$  in spherical coordinates. We illustrate this problem in Figure 18.

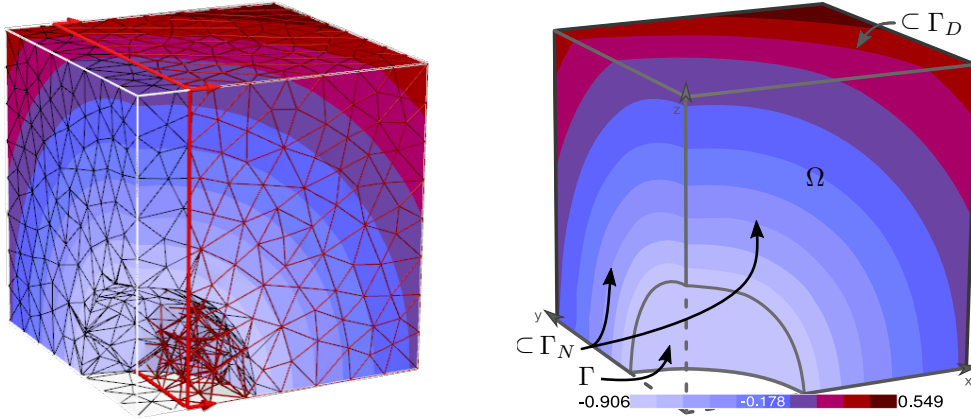
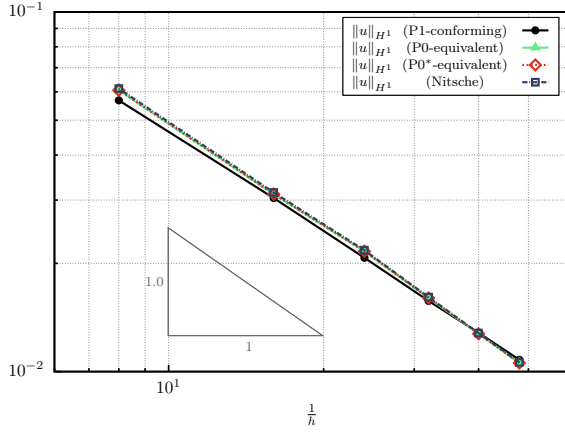
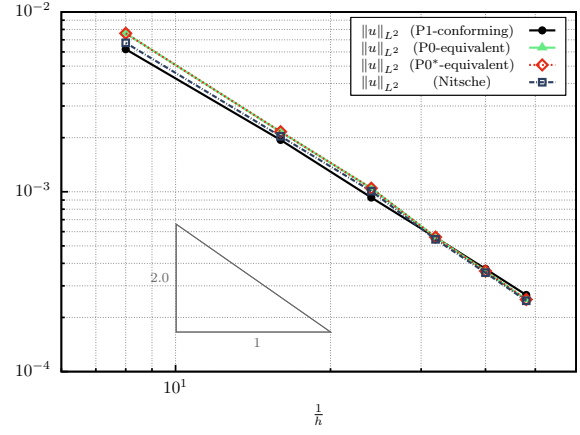
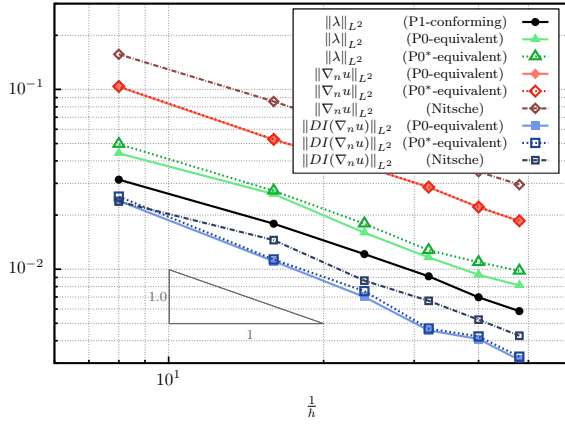
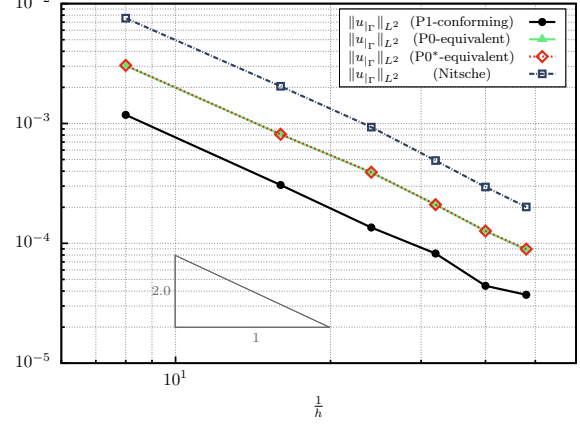
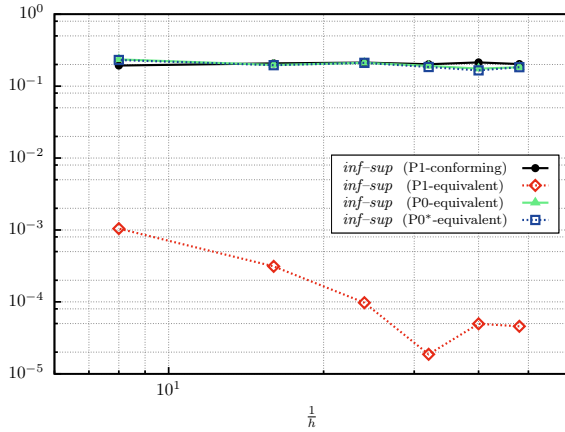
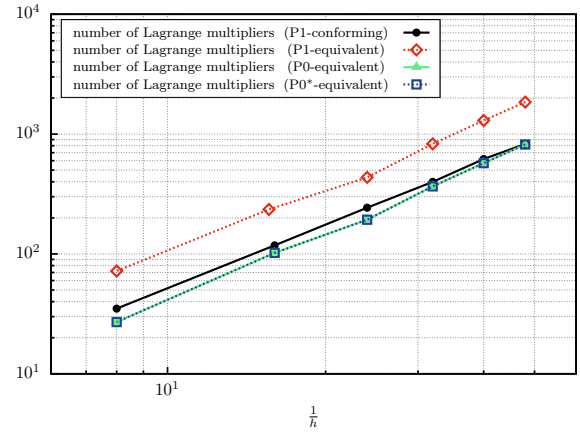


Figure 18: Geometry of the computational domain and exact solution of the Poisson problem, with an embedded spherical surface as Dirichlet boundary.

We carry out a convergence study and report its results in Figure 19.


 (a) Error in the  $H^1$ -norm on the bulk field.

 (b) Error in the  $L^2$ -norm on the bulk field.

 (c) Error in the  $L^2$ -norm on the interfacial flux.

 (d) Error in the  $L^2$ -norm on the interfacial field.


(e) Value of the inf-sup parameter.



(f) Number of Lagrange multipliers.

Figure 19: Convergence study for the Poisson problem with a Dirichlet boundary condition defined on an embedded spherical surface.

Optimal rates of convergence in the  $H^1$ - and  $L^2$ -norms on the bulk field are once again preserved, see Figures 19a and 19b. We find the same behaviour as the previous problem for the interfacial flux in Figure 19c, except using the domain integrals, for which the post-treatment of the Lagrange multipliers is more accurate than with Nitsche's method. Dual approaches lead again to better results on non-conforming mesh for the interfacial field as shown in Figure 19d. Both P0- and P0\*-equivalent spaces achieve a constant inf-sup estimate, which is not the case of the P1-equivalent space, see Figure 19e. This space generates an excessive number of Lagrange multipliers comparing to the P1-conforming space, as shown in Figure 19f. Stable spaces allow to recover FE shape function density.

## 5. Conclusion

A general stable Lagrange multiplier method is proposed in this paper to impose Dirichlet boundary conditions on any embedded boundaries within the context of the extended finite element. The main contributions are the following:

1. A new algorithm is introduced to reduce the Lagrange multiplier space for any codimension of the boundary embedded in a mismatching mesh. One improvement with respect to existing algorithms [18, 66, 48, 44] is its ability to build stable Lagrange multiplier spaces along embedded lines in 3D (codimension two). To our best knowledge, the present work is the first study investigating Dirichlet boundary conditions on this setting within non-conforming meshes. Furthermore, the algorithm is consistent with that proposed in Béchet *et al.* [48] on boundary of codimension one, and benefits of its theoretical proof relating to the inf-sup condition in 2D.
2. Convergence studies are performed on boundary value problems posed on submanifolds of codimension zero or one embedded in 2D or 3D meshes and involving Dirichlet boundary conditions on boundaries of codimension one or two. Using analytical solutions of the problems to determine the errors, the proposed approach shows good accuracy with regard to classical finite element. Optimal rates of convergence are achieved on both the interfacial flux and the primary field on the Dirichlet boundaries.

For each configuration of the space and boundary dimensions, the numerical inf-sup test gives a mesh-independent constant, necessary to the stability of the resulting Lagrange multipliers.

3. Comparisons are presented between our approach and two others introduced in Hautefeuille *et al.* [44] (a Nitsche-type method and a stable Lagrange multiplier method), on problems defined on domains embedded in a mesh of same dimension (codimension zero). Although not essential to the Lagrange multipliers, a domain integral post-processing technique is used to compute accurately the interfacial flux. Results highlight good performance of the newly proposed approach.

In this way, we are able to build a stable Lagrange multiplier space, which is *a priori* compatible with the primal field approximation defined either by using classical P1 shape functions (codimension zero for the model problem) or the P1-equivalent function space introduced in a preliminary paper [14] (codimension one and two).

We obtained a single framework taking advantage of fixed meshes to solve any embedded boundary value problem, without tunable parameter and additional stabilisation term.

Even though the stable Lagrange multiplier method was only applied for Dirichlet boundary conditions in this paper, other problems involving stiff interface conditions may be addressed, e.g. bimaterial interface defined on a membrane in codimension one. Moreover, the large range of configurations supported by the proposed algorithm opens new perspectives in mixed-dimensional coupling with embedded manifolds.

Finally, while the combination of P1- and P0-equivalent spaces allows to handle any boundary value problems of codimension one and two, current efforts are focused on generalising the framework to higher order approximations, e.g. involved in embedded beams or shells with kinematic boundary conditions. This issue will be the subject of a forthcoming paper based on a presentation given at the ECCOMAS Congress 2016.

## Acknowledgements

We are grateful to John Dolbow and Chandrasekhar Annavarapu for providing data sets and fruitful discussions.

## References

- [1] T. Belytschko, Y. Krongauz, D. Organ, M. Fleming, P. Krysl, Meshless methods: An overview and recent developments, *Computer Methods in Applied Mechanics and Engineering* 139 (1-4) (1996) 3–47.
- [2] N. Sukumar, B. Moran, T. Belytschko, The natural element method in solid mechanics, *International Journal for Numerical Methods in Engineering* 43 (5) (1998) 839–887.
- [3] S. Fernández-Méndez, A. Huerta, Imposing essential boundary conditions in mesh-free methods, *Computer Methods in Applied Mechanics and Engineering* 193 (12-14) (2004) 1257–1275.
- [4] I. Babuška, J. Melenk, The partition of unity method, *International Journal for Numerical Methods in Engineering* 40 (4) (1997) 727–758.
- [5] J. Melenk, I. Babuška, The partition of unity finite element method: Basic theory and applications, *Computer Methods in Applied Mechanics and Engineering* 139 (1-4) (1996) 289–314.
- [6] S. Osher, J. A. Sethian, Fronts propagating with curvature dependent speed: Algorithms based on Hamilton-Jacobi formulations, *Journal of Computational Physics* 79 (1) (1988) 12–49.
- [7] J. A. Sethian, Level set methods and fast marching methods: Evolving interfaces in computational geometry, fluid mechanics, computer vision, and materials science, Vol. 3 of *Cambridge monographs on applied and computational mathematics*, Cambridge University Press, Cambridge, UK, 1999.
- [8] T. Belytschko, T. Black, Elastic crack growth in finite elements with minimal remeshing, *International Journal for Numerical Methods in Engineering* 45 (5) (1999) 601–620.
- [9] N. Moës, J. E. Dolbow, T. Belytschko, A finite element method for crack growth without remeshing, *International Journal for Numerical Methods in Engineering* 46 (1) (1999) 131–150.
- [10] N. Sukumar, N. Moës, B. Moran, T. Belytschko, Extended finite element method for three-dimensional crack modelling, *International Journal for Numerical Methods in Engineering* 48 (11) (2000) 1549–1570.
- [11] N. Moës, A. Gravouil, T. Belytschko, Non-planar 3D crack growth by the extended finite element and level sets. Part I: Mechanical model, *International Journal for Numerical Methods in Engineering* 53 (11) (2002) 2549–2568.
- [12] N. Moës, M. Cloirec, P. Cartraud, J.-F. Remacle, A computational approach to handle complex microstructure geometries, *Multiscale Computational Mechanics for Materials and Structures* 192 (28–30) (2003) 3163–3177.

- 
- [13] J. W. Barrett, C. M. Elliott, A finite-element method for solving elliptic equations with Neumann data on a curved boundary using unfitted meshes, *IMA Journal of Numerical Analysis* 4 (3) (1984) 309–325.
  - [14] F. Duboeuf, E. Béchet, Embedded solids of any dimension in the X-FEM. Part I - Building a dedicated P1 function space, *Finite Elements in Analysis and Design* *Submitted*.
  - [15] R. Rangarajan, A. J. Lew, Universal meshes: A method for triangulating planar curved domains immersed in nonconforming meshes, *International Journal for Numerical Methods in Engineering* 98 (4) (2014) 236–264.
  - [16] H. Kabaria, A. J. Lew, Universal meshes for smooth surfaces with no boundary in three dimensions, *International Journal for Numerical Methods in Engineering*.
  - [17] D.-L. Quan, T. Toulorge, E. Marchandise, J.-F. Remacle, G. Bricteux, Anisotropic mesh adaptation with optimal convergence for finite elements using embedded geometries, *Computer Methods in Applied Mechanics and Engineering* 268 (2014) 65–81.
  - [18] N. Moës, E. Béchet, M. Tourbier, Imposing Dirichlet boundary conditions in the extended finite element method, *International Journal for Numerical Methods in Engineering* 67 (12) (2006) 1641–1669.
  - [19] R. Codina, J. Baiges, Approximate imposition of boundary conditions in immersed boundary methods, *International Journal for Numerical Methods in Engineering* 80 (11) (2009) 1379–1405.
  - [20] R. Codina, J. Baiges, Fixed mesh methods in computational mechanics, in: B. Topping, J. Adam, F. Pallarés, R. Bru, M. Romero (Eds.), *Computational Science, Engineering & Technology Series*, Vol. 26, Saxe-Coburg Publications, Stirlingshire, UK, 2010, pp. 81–102.
  - [21] S. Soghrati, A. M. Aragón, C. Armando Duarte, P. H. Geubelle, An interface-enriched generalized FEM for problems with discontinuous gradient fields, *International Journal for Numerical Methods in Engineering* 89 (8) (2012) 991–1008.
  - [22] S. Soghrati, P. H. Geubelle, A 3D interface-enriched generalized finite element method for weakly discontinuous problems with complex internal geometries, *Computer Methods in Applied Mechanics and Engineering* 217–220 (2012) 46–57.
  - [23] A. C. Cuba Ramos, A. M. Aragón, S. Soghrati, P. H. Geubelle, J.-F. Molinari, A new formulation for imposing Dirichlet boundary conditions on non-matching meshes, *International Journal for Numerical Methods in Engineering* 103 (6) (2015) 430–444.
  - [24] S. Soghrati, Hierarchical interface-enriched finite element method: An automated technique for mesh-independent simulations, *Journal of Computational Physics* 275 (2014) 41–52.
  - [25] P. W. Hemker, W. Hoffman, R. M. H. Van, Discontinuous Galerkin discretization with embedded boundary conditions, *Computational Methods in Applied Mathematics Comput. Methods Appl. Math.* 3 (1) (2003) 135–158.
  - [26] M. van Raalte, A feasibility study for discontinuous Galerkin discretization with embedded Dirichlet

- 
- boundary condition, *Applied Numerical Mathematics* 51 (2-3) (2004) 361–383.
- [27] A. J. Lew, G. C. Buscaglia, A discontinuous-Galerkin-based immersed boundary method, *International Journal for Numerical Methods in Engineering* 76 (4) (2008) 427–454.
  - [28] R. Rangarajan, A. Lew, G. C. Buscaglia, A discontinuous-Galerkin-based immersed boundary method with non-homogeneous boundary conditions and its application to elasticity, *Computer Methods in Applied Mechanics and Engineering* 198 (17-20) (2009) 1513–1534.
  - [29] A. Gerstenberger, W. A. Wall, An embedded Dirichlet formulation for 3D continua, *International Journal for Numerical Methods in Engineering* 82 (5) (2010) 537–563.
  - [30] J. Baiges, R. Codina, F. Henke, S. Shahmiri, W. A. Wall, A symmetric method for weakly imposing Dirichlet boundary conditions in embedded finite element meshes, *International Journal for Numerical Methods in Engineering* 90 (5) (2012) 636–658.
  - [31] R. Codina, J. Baiges, Weak imposition of essential boundary conditions in the finite element approximation of elliptic problems with non-matching meshes, *International Journal for Numerical Methods in Engineering* 104 (7) (2015) 624–654.
  - [32] S. Kollmannsberger, A. Özcan, J. Baiges, M. Ruess, E. Rank, A. Reali, Parameter-free, weak imposition of Dirichlet boundary conditions and coupling of trimmed patches, *International Journal for Numerical Methods in Engineering* 101 (9) (2015) 670–699.
  - [33] C. S. Peskin, Flow patterns around heart valves: A numerical method, *Journal of Computational Physics* 10 (2) (1972) 252–271.
  - [34] R. LeVeque, Z. Li, The immersed interface method for elliptic equations with discontinuous coefficients and singular sources, *SIAM Journal on Numerical Analysis* 31 (4) (1994) 1019–1044.
  - [35] R. LeVeque, Z. Li, Immersed interface methods for Stokes flow with elastic boundaries or surface tension, *SIAM Journal on Scientific Computing* 18 (3) (1997) 709–735.
  - [36] L. Lee, R. LeVeque, An immersed interface method for incompressible Navier–Stokes equations, *SIAM Journal on Scientific Computing* 25 (3) (2003) 832–856.
  - [37] S. Xu, Z. J. Wang, An immersed interface method for simulating the interaction of a fluid with moving boundaries, *Journal of Computational Physics* 216 (2) (2006) 454–493.
  - [38] I. Babuška, The finite element method with penalty, *Mathematics of Computation* 27 (122) (1973) 221–228.
  - [39] J. W. Barrett, C. M. Elliott, Finite element approximation of the Dirichlet problem using the boundary penalty method, *Numerische Mathematik* 49 (4) (1986) 343–366.
  - [40] J. Nitsche, Über ein Variationsprinzip zur Lösung von Dirichlet-Problemen bei Verwendung von Teilräumen, die keinen Randbedingungen unterworfen sind, *Abhandlungen aus dem Mathematischen Seminar der Universität Hamburg* 36 (1) (1971) 9–15.

- 
- [41] M. Juntunen, R. Stenberg, Nitsche's method for general boundary conditions, *Mathematics of Computation* 78 (267) (2009) 1353–1374.
  - [42] G. Dupire, J. Boufflet, M. Dambrine, P. Villon, On the necessity of Nitsche term, *Applied Numerical Mathematics* 60 (9) (2010) 888–902.
  - [43] J. Boufflet, M. Dambrine, G. Dupire, P. Villon, On the necessity of Nitsche term. Part II: An alternative approach, *Applied Numerical Mathematics* 62 (5) (2012) 521–535.
  - [44] M. Hautefeuille, C. Annavarapu, J. E. Dolbow, Robust imposition of Dirichlet boundary conditions on embedded surfaces, *International Journal for Numerical Methods in Engineering* 90 (1) (2012) 40–64.
  - [45] J. Dolbow, I. Harari, An efficient finite element method for embedded interface problems, *International Journal for Numerical Methods in Engineering* 78 (2) (2009) 229–252.
  - [46] A. Embar, J. Dolbow, I. Harari, Imposing Dirichlet boundary conditions with Nitsche's method and spline-based finite elements, *International Journal for Numerical Methods in Engineering* (2010) n/a–n/a.
  - [47] H. Ji, J. E. Dolbow, On strategies for enforcing interfacial constraints and evaluating jump conditions with the extended finite element method, *International Journal for Numerical Methods in Engineering* 61 (14) (2004) 2508–2535.
  - [48] E. Béchet, N. Moës, B. Wohlmuth, A stable Lagrange multiplier space for stiff interface conditions within the extended finite element method, *International Journal for Numerical Methods in Engineering* 78 (8) (2009) 931–954.
  - [49] J. Haslinger, Y. Renard, A new fictitious domain approach inspired by the extended finite element method, *SIAM J. Numer. Anal.* 47 (2) (2009) 1474–1499.
  - [50] O. A. Ladyzhenskaya, The mathematical theory of viscous incompressible flow, Vol. 2 of *Mathematics and its Applications*, 2d English ed., rev. and enl. Translated from the Russian by Richard A. Silverman and John Chu. Gordon and Breach Science Publishers, New York, 1969.
  - [51] I. Babuška, Error-bounds for finite element method, *Numerische Mathematik* 16 (4) (1971) 322–333.
  - [52] I. Babuška, The finite element method with Lagrangian multipliers, *Numerische Mathematik* 20 (3) (1973) 179–192.
  - [53] F. Brezzi, On the existence, uniqueness and approximation of saddle-point problems arising from lagrangian multipliers, *ESAIM: Mathematical Modelling and Numerical Analysis - Modélisation Mathématique et Analyse Numérique* 8 (R2) (1974) 129–151.
  - [54] F. Brezzi, L. P. Franca, D. Marini, A. Russo, Stabilization techniques for domain decomposition methods with non-matching grids, in: P. E. Bjørstad, M. S. Espedal, D. E. Keyes (Eds.), *Proceedings of the Ninth International Conference on Domain Decomposition Method*, Domain Decomposition Press, Bergen, 1998, pp. 1–11.
  - [55] H. M. Mourad, J. Dolbow, I. Harari, A bubble-stabilized finite element method for Dirichlet constraints

- on embedded interfaces, *International Journal for Numerical Methods in Engineering* 69 (4) (2007) 772–793.
- [56] J. Dolbow, L. Franca, Residual-free bubbles for embedded Dirichlet problems, *Computer Methods in Applied Mechanics and Engineering* 197 (45–48) (2008) 3751–3759.
- [57] J. D. Sanders, J. E. Dolbow, T. A. Laursen, On methods for stabilizing constraints over enriched interfaces in elasticity, *International Journal for Numerical Methods in Engineering* 78 (9) (2009) 1009–1036.
- [58] H. J. Barbosa, T. J. R. Hughes, The finite element method with Lagrange multipliers on the boundary: circumventing the Babuška-Brezzi condition, *Computer Methods in Applied Mechanics and Engineering* 85 (1) (1991) 109–128.
- [59] H. J. C. Barbosa, T. J. R. Hughes, Boundary Lagrange multipliers in finite element methods: Error analysis in natural norms, *Numerische Mathematik* 62 (1) (1992) 1–15.
- [60] R. Stenberg, On some techniques for approximating boundary conditions in the finite element method, *Proceedings of the International Symposium on Mathematical Modelling and Computational Methods Modelling* 94 63 (1–3) (1995) 139–148.
- [61] E. Burman, P. Hansbo, Fictitious domain finite element methods using cut elements: I. A stabilized Lagrange multiplier method, *Computer Methods in Applied Mechanics and Engineering* 199 (41–44) (2010) 2680–2686.
- [62] E. Burman, Projection stabilization of Lagrange multipliers for the imposition of constraints on interfaces and boundaries: Projection Stabilization Of Lagrange Multipliers, *Numerical Methods for Partial Differential Equations* 30 (2) (2014) 567–592.
- [63] S. Amdouni, M. Moakher, Y. Renard, A local projection stabilization of fictitious domain method for elliptic boundary value problems, *Applied Numerical Mathematics* 76 (0) (2014) 60–75.
- [64] R. Glowinski, T.-W. Pan, J. Periaux, A fictitious domain method for Dirichlet problem and applications, *Computer Methods in Applied Mechanics and Engineering* 111 (3–4) (1994) 283–303.
- [65] V. Girault, R. Glowinski, Error analysis of a fictitious domain method applied to a Dirichlet problem, *Japan Journal of Industrial and Applied Mathematics* 12 (3) (1995) 487–514.
- [66] S. Geniaut, P. Massin, N. Moës, A stable 3D contact formulation using X-FEM, *European Journal of Computational Mechanics* 16 (2) (2007) 259–275.
- [67] I. Nistor, M. L. E. Guiton, P. Massin, N. Moës, S. Géniaut, An X-FEM approach for large sliding contact along discontinuities, *International Journal for Numerical Methods in Engineering* 78 (12) (2009) 1407–1435.
- [68] M. Olshanskii, A. Reusken, J. Grande, A finite element method for elliptic equations on surfaces, *SIAM Journal on Numerical Analysis* 47 (5) (2009) 3339–3358.

- [69] S. Amdouni, P. Hild, V. Lleras, M. Moakher, Y. Renard, A stabilized Lagrange multiplier method for the enriched finite-element approximation of contact problems of cracked elastic bodies, *ESAIM: Mathematical Modelling and Numerical Analysis* 46 (04) (2012) 813–839.
- [70] D. Chapelle, K. Bathe, The inf-sup test, *Computers & Structures* 47 (4-5) (1993) 537–545.
- [71] K.-J. Bathe, The inf-sup condition and its evaluation for mixed finite element methods, *Computers & Structures* 79 (2) (2001) 243–252.
- [72] E. Burman, P. Hansbo, M. G. Larson, K. Larsson, A. Massing, Finite element approximation of the Laplace-Beltrami operator on a surface with boundary, *arXiv:1509.08597*(2015).
- [73] I. Babuška, Approximation by Hill functions. II., *Commentationes Mathematicae Universitatis Carolinae* 13 (1) (1972) 1–22.